Biochemistry of capacitation

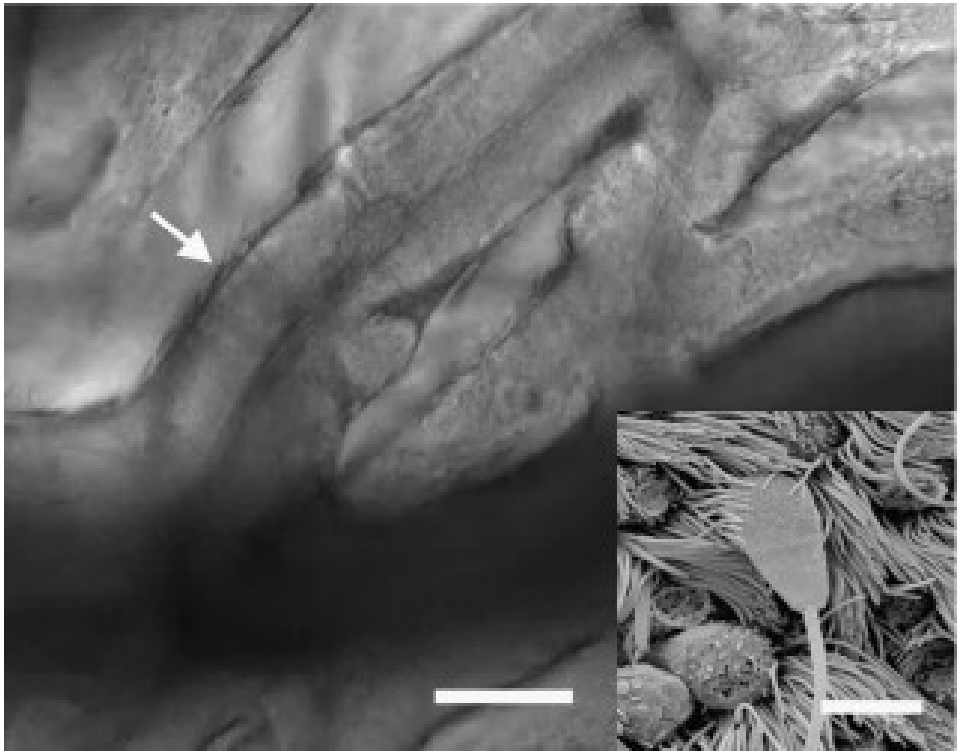

Main aspects of capacitation

- There are important differences between in vitro and in vivo capacitation.
- It involves several different sperm populations.
- It does not exist a reliable molecular marker of capacitation.
- The signaling strategy is based on redundant mechamisms.

Membrane potential

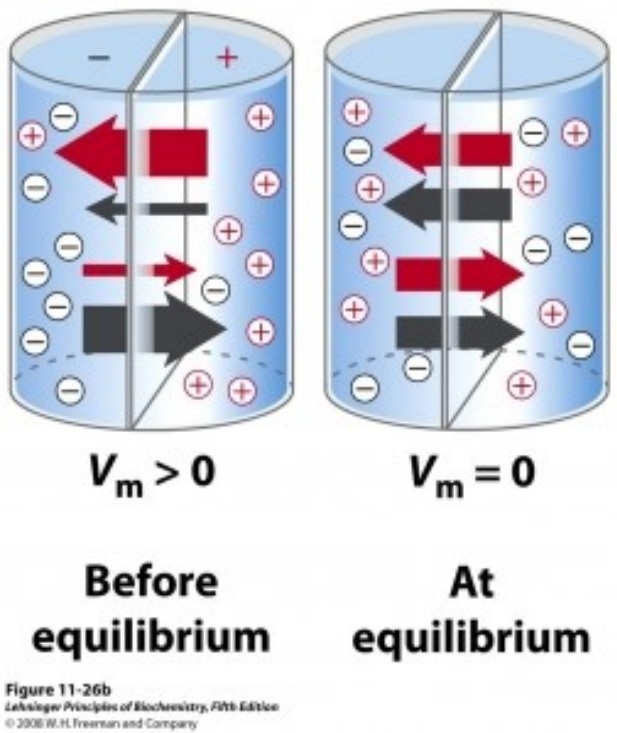

Figure 11-26b
Lehninger Principles of Biochemistry, Fifth Edition

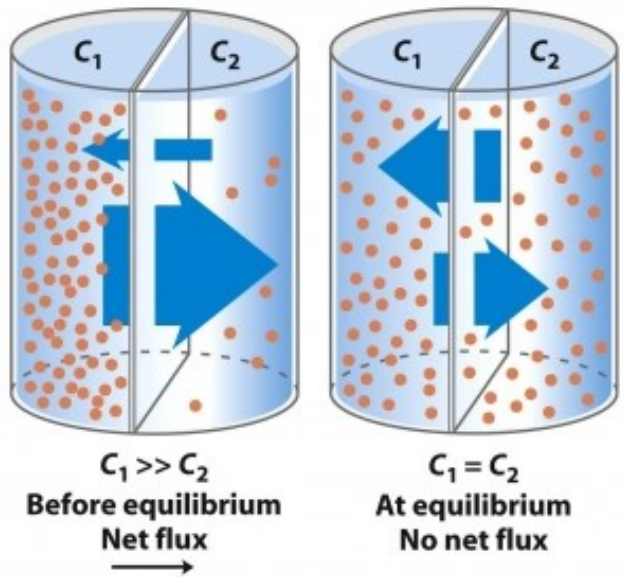

Figure 11-26a
Lehninger Principles of Biochemistry, Fifth Edition

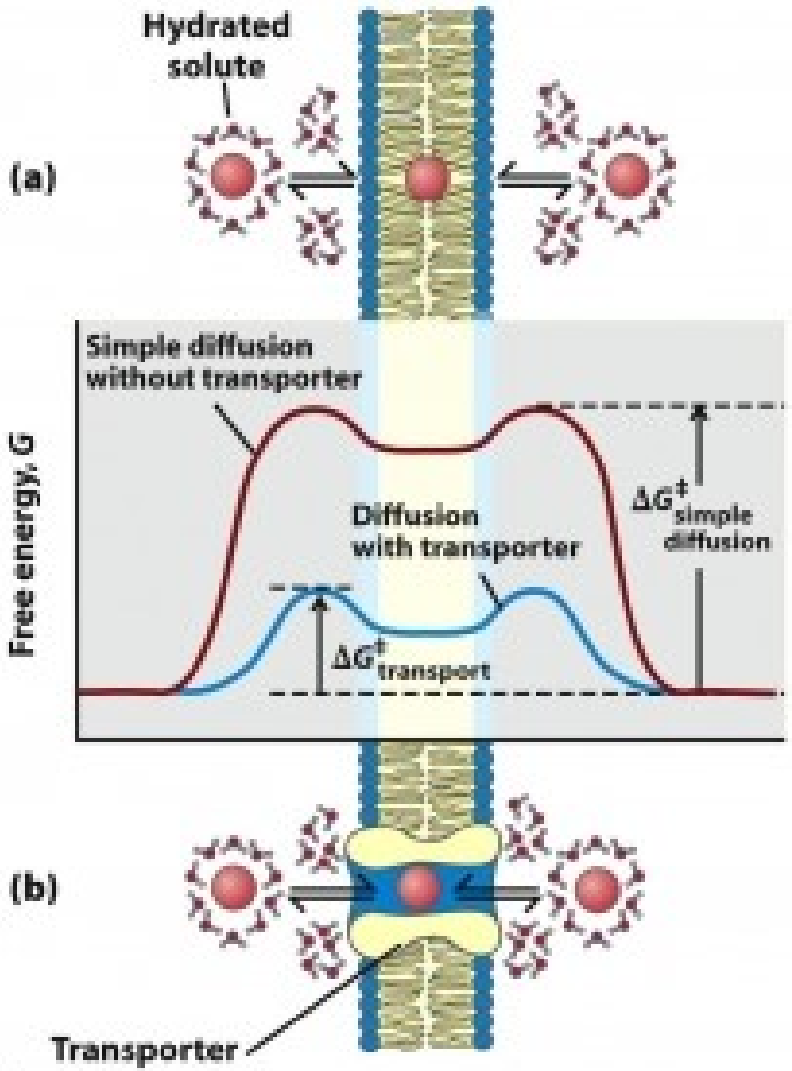

Figure 11-27
Lehninger Principles of Biochemistry, Fifth Edition

Sodium-Potassium Pump — Steps 1–3

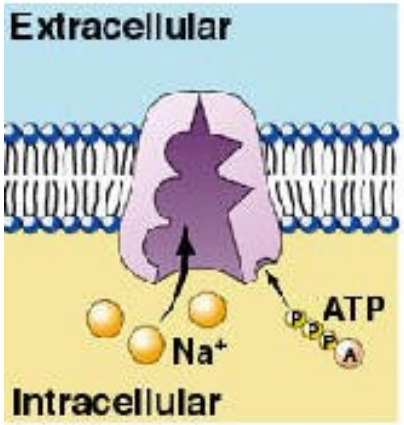

1. Protein in membrane binds intracellular sodium.

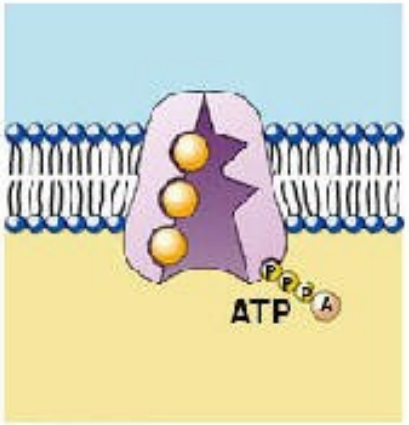

2. ATP phosphorylates protein with bound sodium.

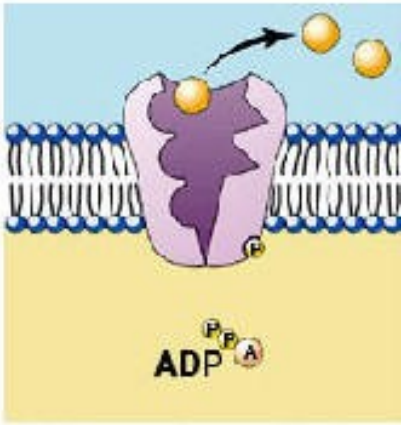

3. Phosphorylation causes conformational change in protein, allowing sodium to leave.

Sodium-Potassium Pump — Steps 4–6

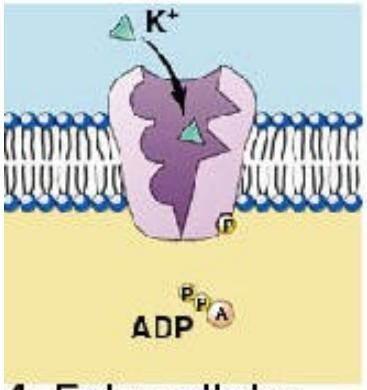

4. Extracellular potassium binds to exposed sites.

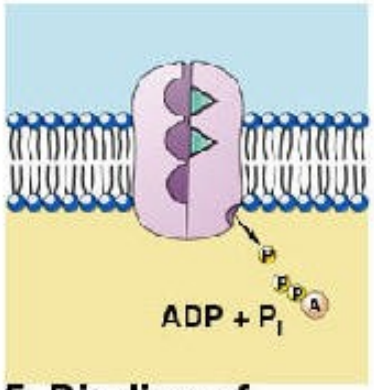

5. Binding of potassium causes dephos-phorylation of protein.

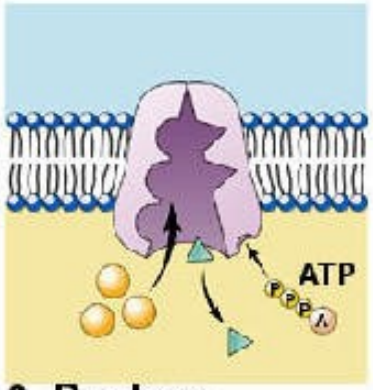

6. Dephos-phorylation of protein triggers change back to original conformation, potassium moves into cell, and the cycle repeats.

Calcium signaling in spem capacitation

Calcium clearance :

- Plasma Membrane Ca^{2+}ATPase (PMCA): it exports 1 Ca^{2+} and it imports 1 or 2 H^+, at ATP expense. It is constitutively active.

- Na^+/Ca^{2+} exchanger (NCX): it exposrts 1 Ca^{2+} and in imports 3 Na^+. It works accrding to the Na^+ gradient, when $[Ca^{2+}]_i$ rises.

- sarcoplasmic-endoplasmic reticulum Ca^{2+}/ATPase (SERCA):imports/exposrts Ca^{2+} from intracellular stores.

- mitochondrial Ca^{2+} uniporter (MCU): it imports Ca^{2+} in mitochondra, when $[Ca^{2+}]_i > 450$ nM.

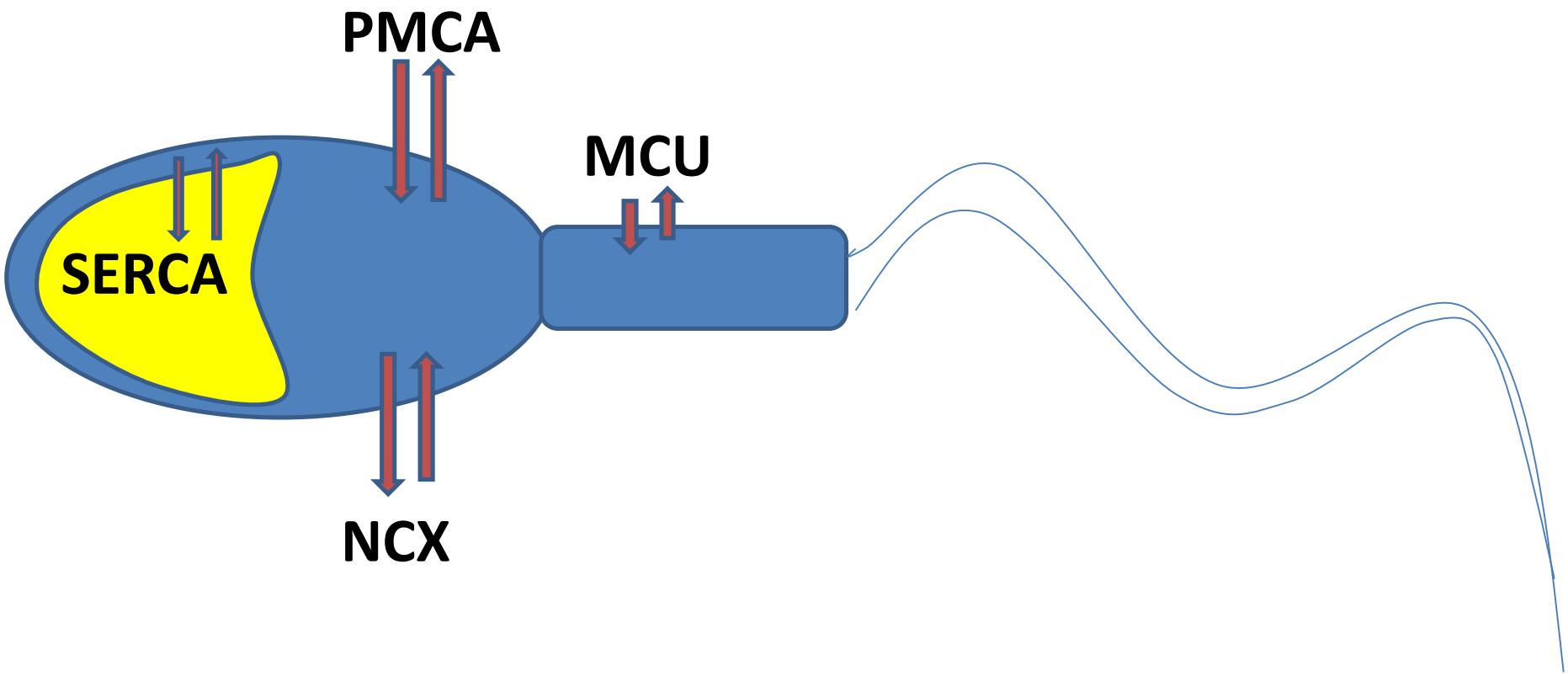
PMCA
MCU
SERCA
NCX

SERCA pumps

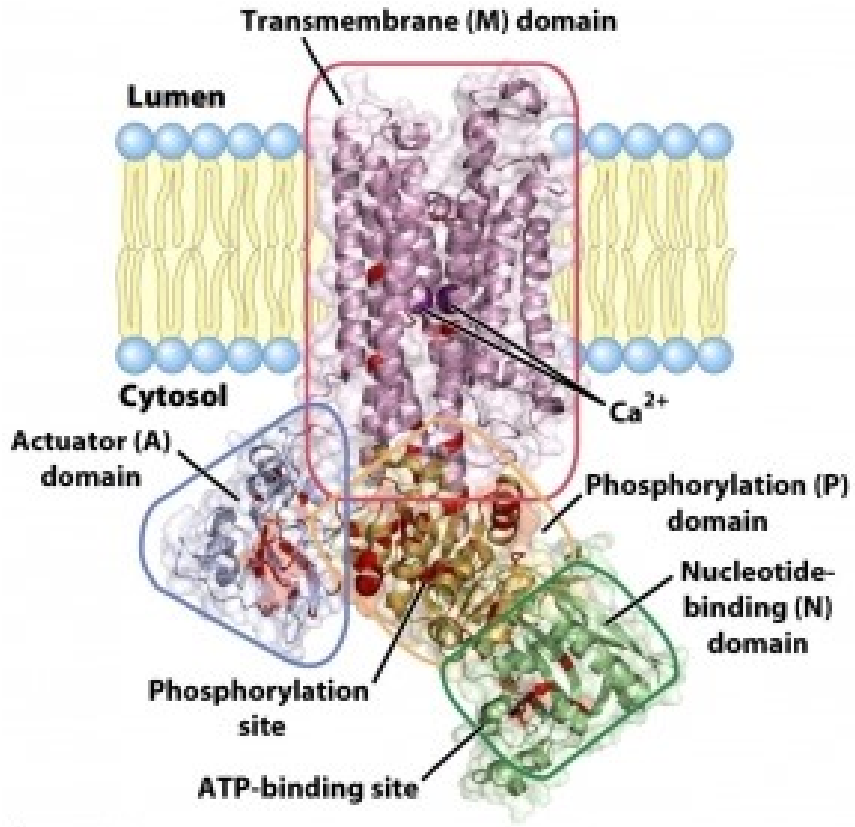

Figure 11-35
Lehninger Principles of Biochemistry, Fifth Edition

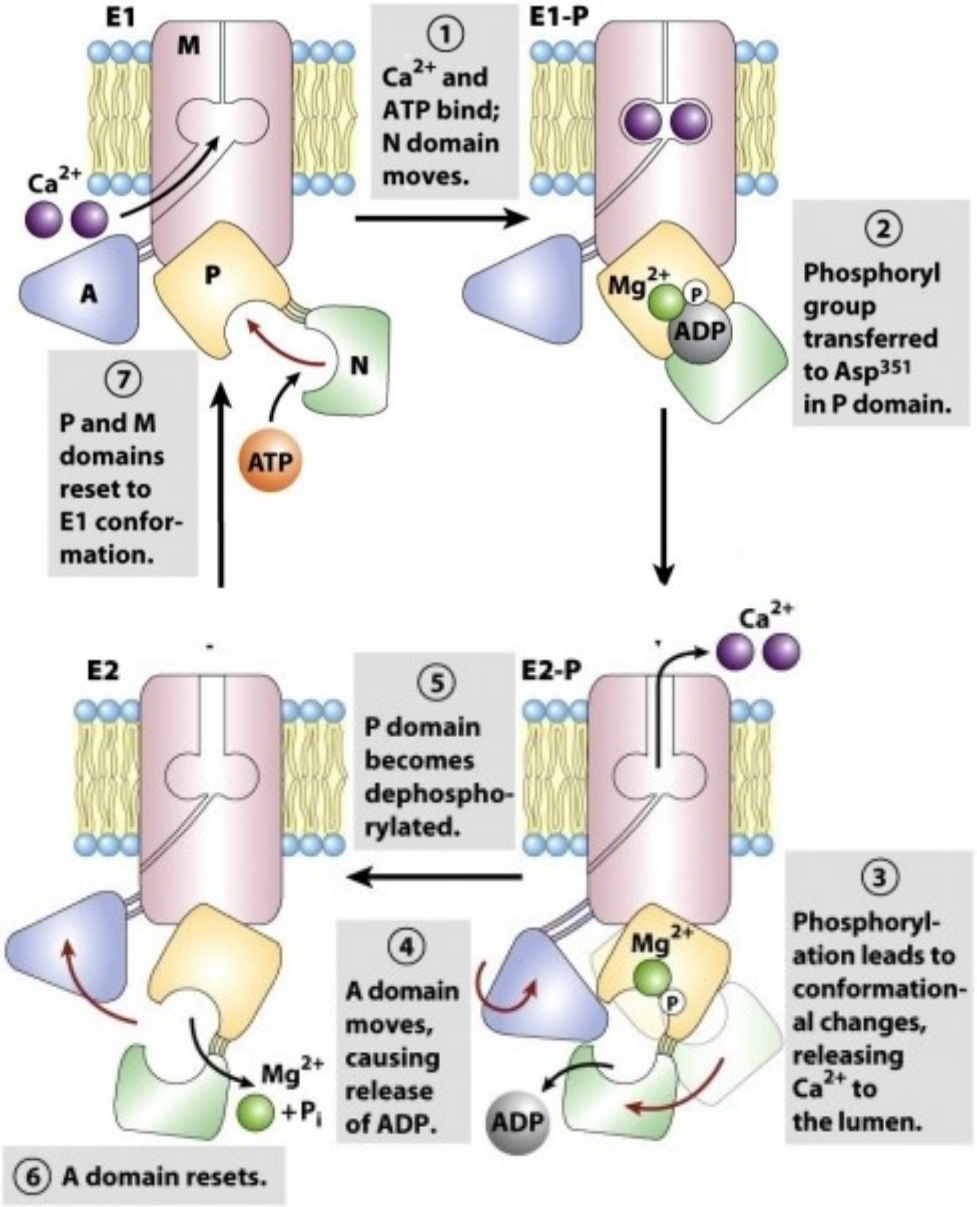

Figure 11-36

Lehninger Principles of Biochemistry, Fifth Edition

Redundant Nuclear Envelope (RNE)

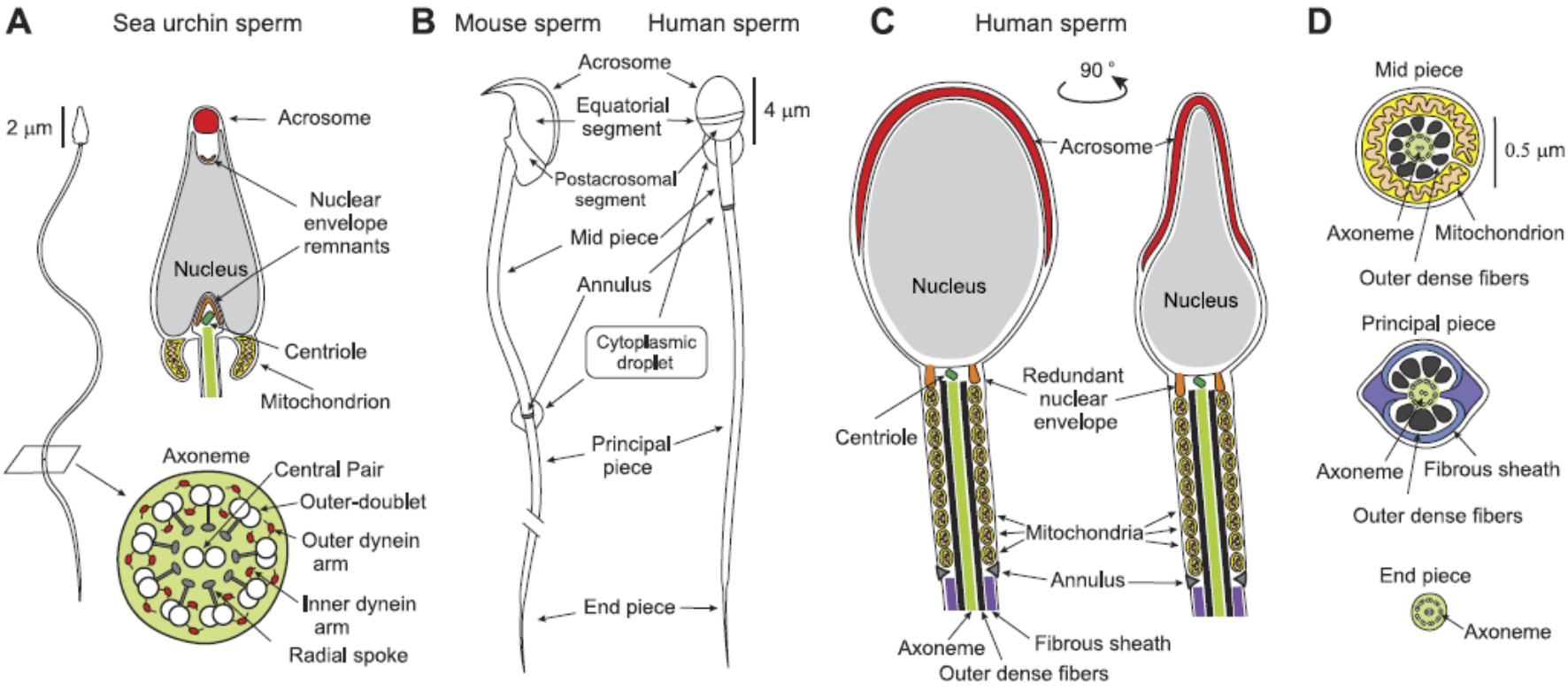

Calcium channels

- voltage-gated Ca2+ (CaV) channels
- transient receptor potential-(TRP) channels
- and cyclic nucleotide-gated- (CNG) channels
- CatSper

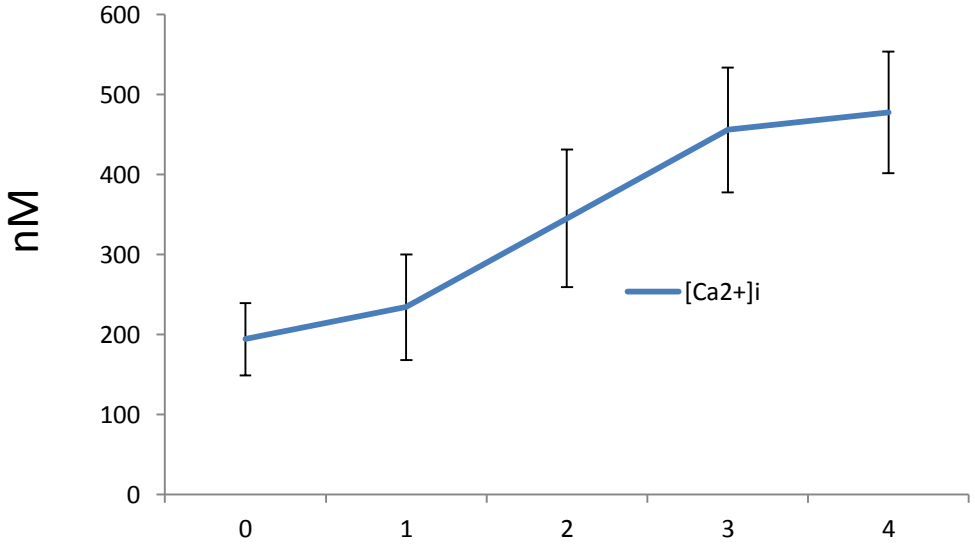

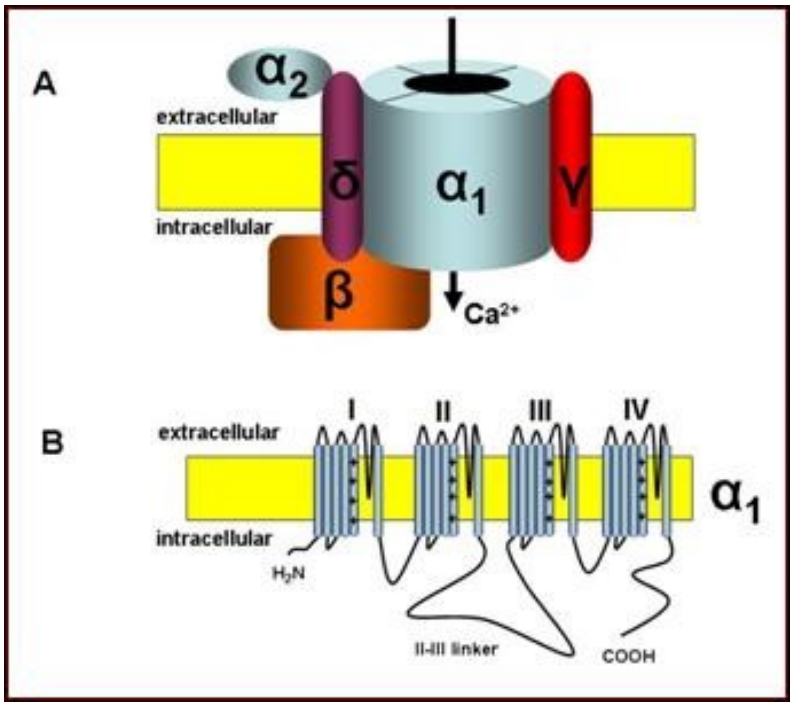

During capacitation sperm membrane hyperpolarizes (in mouse from -50 to -80 mM). As the membrane potential lowers, the probability that the channels open increases.

CaV

Current Type	1,4-dihydropyridine sensitivity (DHP)	ω-conotoxin sensitivity (ω-CTX)	ω-agatoxin sensitivity (ω-AGA)
L-type	blocks	resistant	resistant
N-type	resistant	blocks	resistant
P/Q-type	resistant	resistant	blocks
R-type	resistant	resistant	resistant

Type	Voltage	α_1 subunit (gene name)	Associated subunits	Most often found in
L-type calcium channel("Long-Lasting" AKA "DHP Receptor")	HVA (high voltage activated)	$Ca_v1.1$(*CACNA1S*) $Ca_v1.2$(*CACNA1C*)$Ca_v1.3$(*CACNA 1D*) $Ca_v1.4$(*CACNA1F*)	$\alpha_2\delta$, β, γ	Skeletal muscle, smooth muscle, bone (osteoblasts), ventricular myocytes** (responsible for prolonged action potential in cardiac cell; also termed DHP receptors), dendrites and dendritic spines of cortical neurones
P-type calcium channel("Purkinje") /Q-type calcium channel	HVA (high voltage activated)	$Ca_v2.1$(*CACNA1A*)	$\alpha_2\delta$, β, possibly γ	Purkinje neurons in the cerebellum / Cerebellar granule cells
N-type calcium channel("Neural"/"Non-L")	HVA (high-voltage-activated)	$Ca_v2.2$(*CACNA1B*)	$\alpha_2\delta/\beta_1$, β_3, β_4, possibly γ	Throughout the brain and peripheral nervous system.
R-type calcium channel("Residual")	intermediate-voltage-activated	$Ca_v2.3$(*CACNA1E*)	$\alpha_2\delta$, β, possibly γ	Cerebellar granule cells, other neurons
T-type calcium channel("Transient")	low-voltage-activated	$Ca_v3.1$(*CACNA1G*) $Ca_v3.2$(*CACNA1H*) $Ca_v3.3$(*CACNA1I*)		neurons, cells that have pacemaker activity, bone (osteocytes)

Table 1. Expression of Ca_v channels in sperm cells

Channel	mRNA	WB	ICC	Detectable	Mice KO	Reference Nos.
$Ca_v1.1$					Die at birth	288
$Ca_v1.2$	Mo Hu Su	Mo Su	Mo (h,pp) Hu (mp) Su (f)		Lethal	164, 219, 223, 288, 400, 514, 556
$Ca_v1.3$					fertile	413
$Ca_v1.4$					Retinal defects	342
$Ca_v2.1$	Mo	Mo	Mo (h,f)		Die at 1 month	288, 324, 556
$Ca_v2.2$	Hu	Mo	Mo (h,pp)	Spermatogenic	Fertile	272, 400, 554
$Ca_v2.3$	Mo Hu Su	Mo Su	Mo (h,pp) Hu (pp,h) Su (h, f)	Spermatogenic	Fertile	223, 324, 514, 556
$Ca_v3.1$	Mo Hu		Mo (h,f) Hu (mp,h)		Fertile	134, 164, 400, 479, 514
$Ca_v3.2$	Mo Hu		Mo (h) Hu (f)	Spermatogenic Testicular sperm	Fertile	114, 134, 164, 400, 478, 514
$Ca_v3.3$	Mo		Mo (mp) Hu (mp)		NA	134, 400, 514
Catsper 1	Mo Hu	Mo	Mo (pp)	Epididymal sperm	Infertile	292, 432
Catsper 2	Mo Hu	Mo	Mo (pp)		Infertile	425
Catsper 3	Mo Hu	Mo	Mo (f,h)		Infertile	278, 335, 423
Catsper 4	Mo Hu	Mo	Mo (f,h)		Infertile	278, 335, 423

The detection of the mRNA, the protein by Western blot (WB), or the subcellular localization (h, head; f, flagella; pp, principal piece; mp, midpiece) by immunocytochemistry (ICC) for each CaV subunit and different species is shown. The detection of the specific current (if present) and the knockout (KO) phenotype (Mo, mouse; Hu, human; Su, sea urchin) is indicated. NA, not available.

Control mechanisms

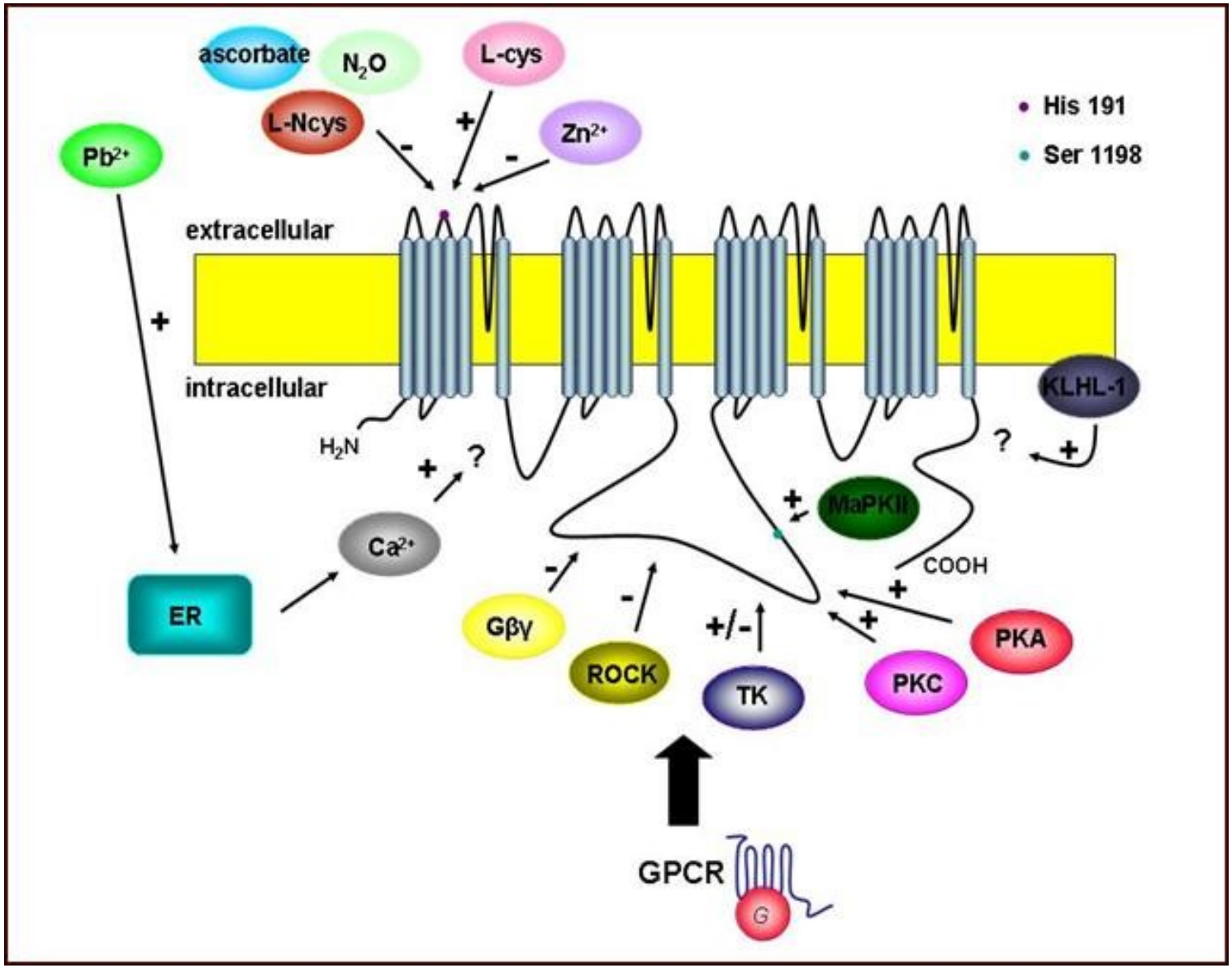

CNG channels

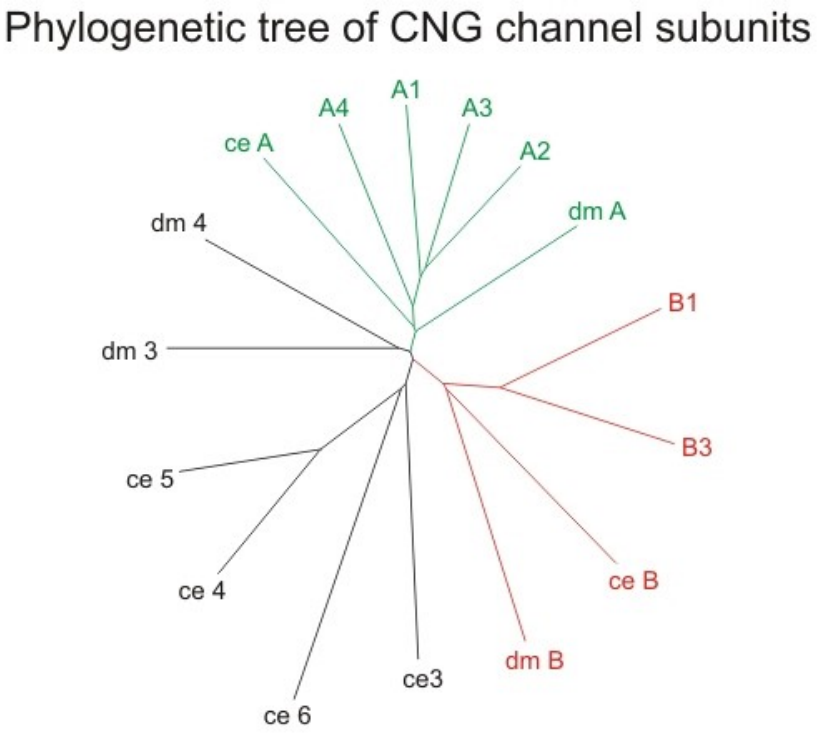

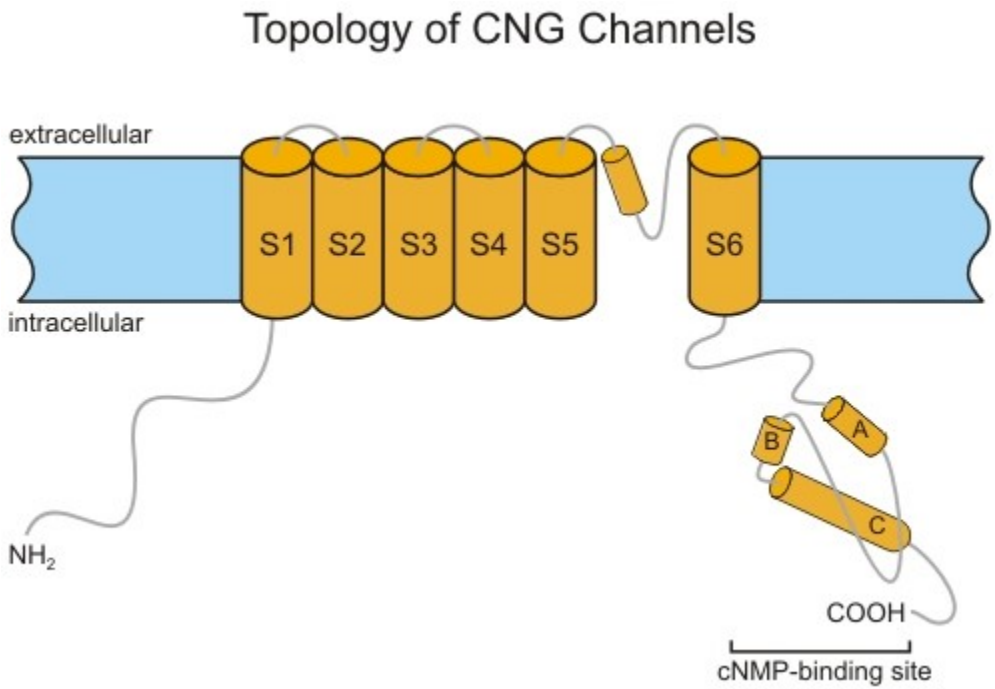

Chemiotassi in riccio di mare

TRP channels

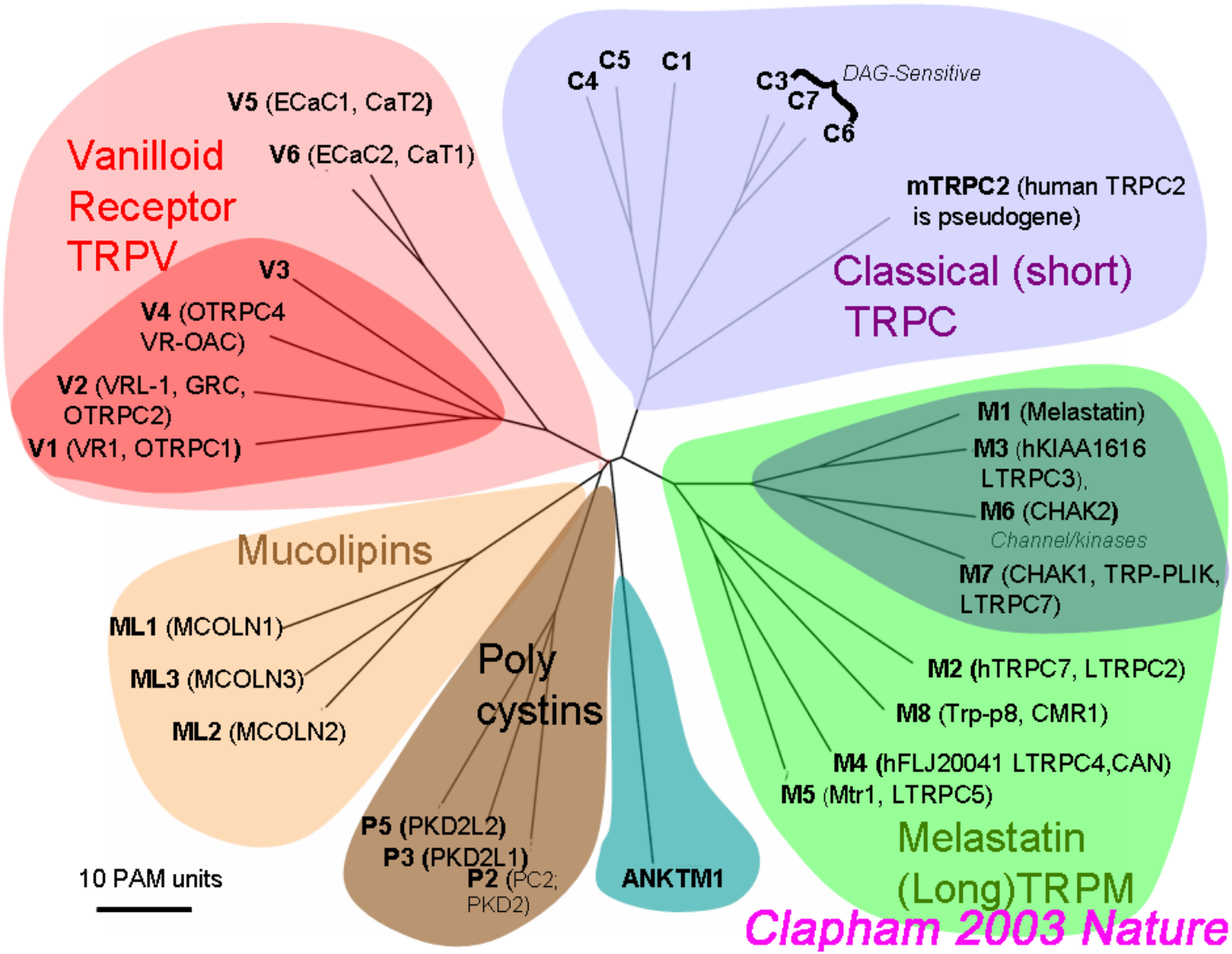

Table 3. Expression of TRP and intracellular channels in sperm cells

Channel	mRNA	WB	ICC	Reference Nos.
IP_3R	Mo	Mo Rt Ha Do	Mo (h) Rt (h) Ha (h) Do (h)	515, 539
RyR	Mo		Mo (h,f) Hu (h)	119, 239, 515
TRPC1	Mo Hu		Mo (f) Hu (f)	85, 516
TRPC2	Mo		Mo (h)	283, 516
TRPC3	Mo Hu		Mo (h,f) Hu (h,f)	85, 516
TRPC4	Mo			516
TRPC5	Mo			514
TRPC6	Mo Hu		Mo (h,f) Hu (h,f)	85, 516
TRPC7	Mo Hu			85, 516
TRPM3	Rt			318
TRPM4	Rt			318
TRPM7	Rt			318
TRPM8	Hu	Hu	Hu (h,f)	143, 347
TRPV1	Rt Bo			49, 50, 319
TRPV5	Rt			318

The detection of the mRNA, the protein by Western blot (WB), or the subcellular localization (h, head; f, flagella) by immunocytoche mistry (ICC) of each channel and different species (Mo, mouse; Hu, human; Rt, rat; Bo, boar; Ha, hamster; Do, dog) is indicated. Detailed information about transient receptor potential (TRP) knockout phenotypes can be found in Reference 562.

TRPV1

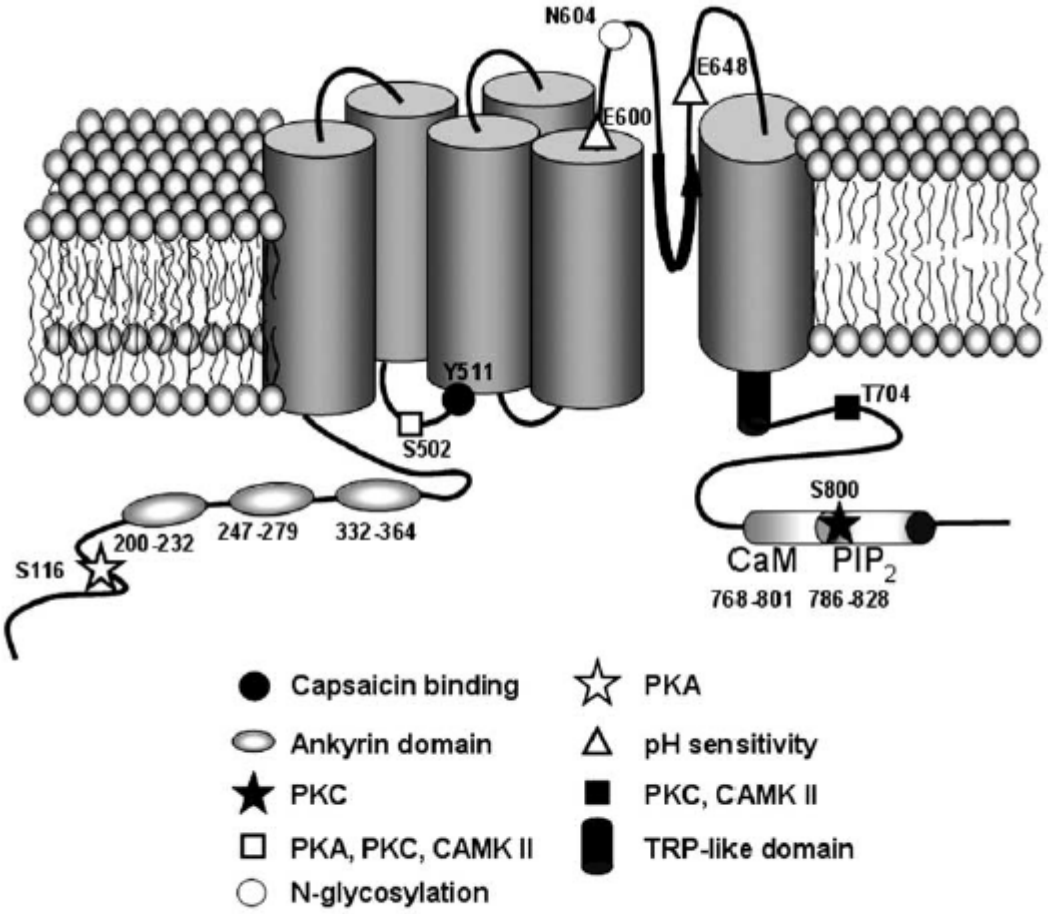

Fig. 1. Topological organization of a TRPV1 channel subunit. The model consist of an N-terminal domain (amino acids 1–414) containing three ankyrin domains and a phosphorylation site for protein kinase A; six transmembrane-spanning segments (cylinders) and a large stretch connecting the S5 and S6 membrane segments that hold a short amphipathic fragment (curved arrow); and a cytosolic C-terminus domain carrying calmodulin (CaM) and phosphatydylinositol-4,5-bisphosphate (PIP_2) binding sites. Highlighted are molecular determinants of TRPV1 properties. Numbers denote the amino acid number in the deduced rat primary sequence.

Polymodal sensors

- Temperature
- pH
- Nociception

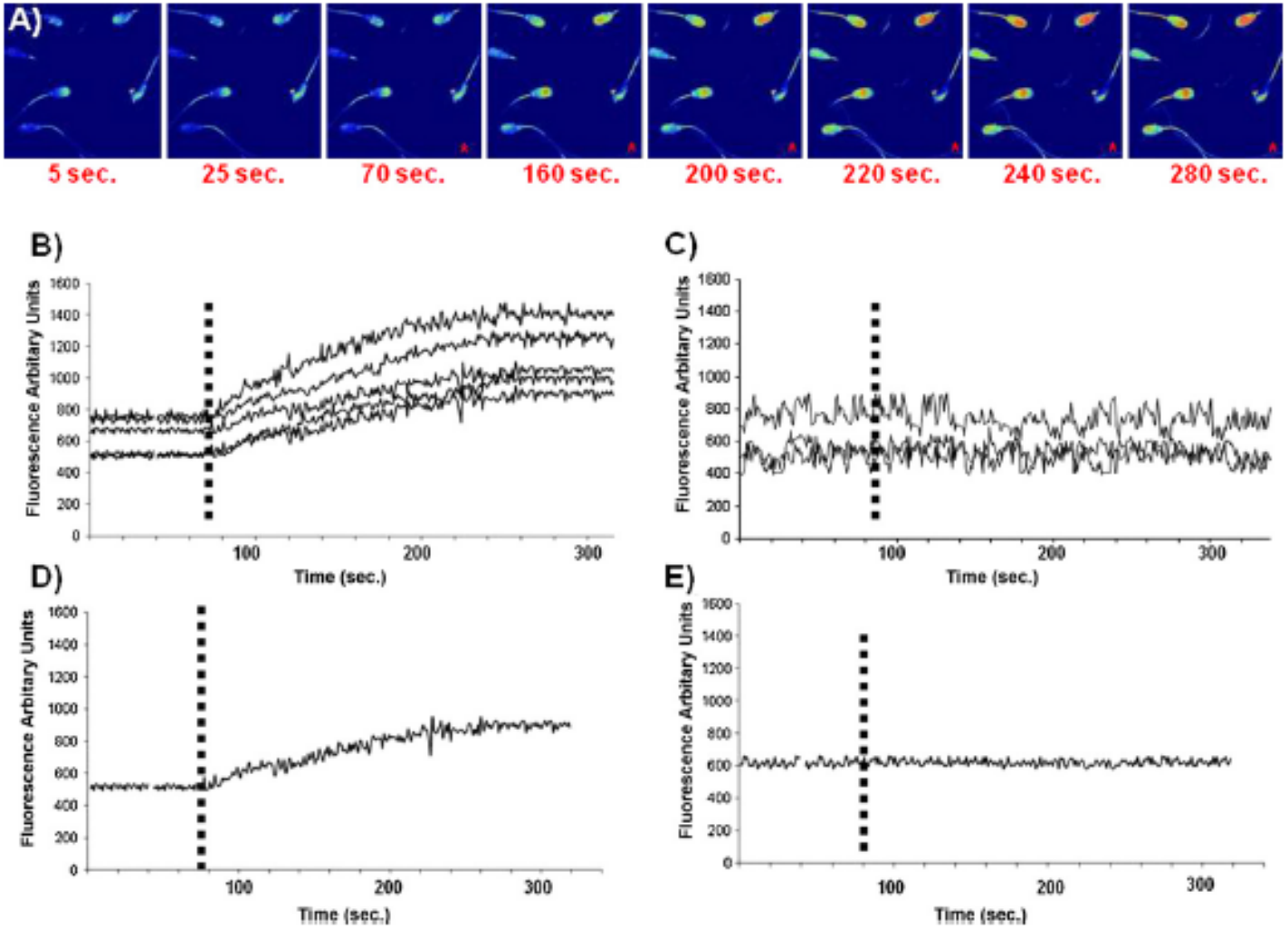

Fig. 2. (A) Confocal image gallery of bis-oxonol loaded spermatozoa exposed to CPS (asterisk). The pseudo-colour scale from blue to white represents the increasing emission intensity, expressed as Fluorescence Arbitrary Units. Since bis oxinol is a negatively charged probe the rise in sperm cell fluorescence observed after <10 s to the addition of CPS reveals a depolarization in sperm resting transmembrane potential. (B) Effect of CPS (vertical black dot line) on the membrane polarity of five sperm cells. (C) Effect of CPS (vertical black dot line) on the membrane polarity of three different sperm cells recorded in Na^+ free medium (choline chloride). (D) Effect of CPS (vertical black dot line) on the membrane polarity of one sperm cell recorded in TTX-treated spermatozoa. (E) Effect of CPZ (vertical black dot line) on the membrane polarity of one sperm cell recorded in control condition. (For interpretation of the references to colour in this figure legend, the reader is referred to the web version of the article.)

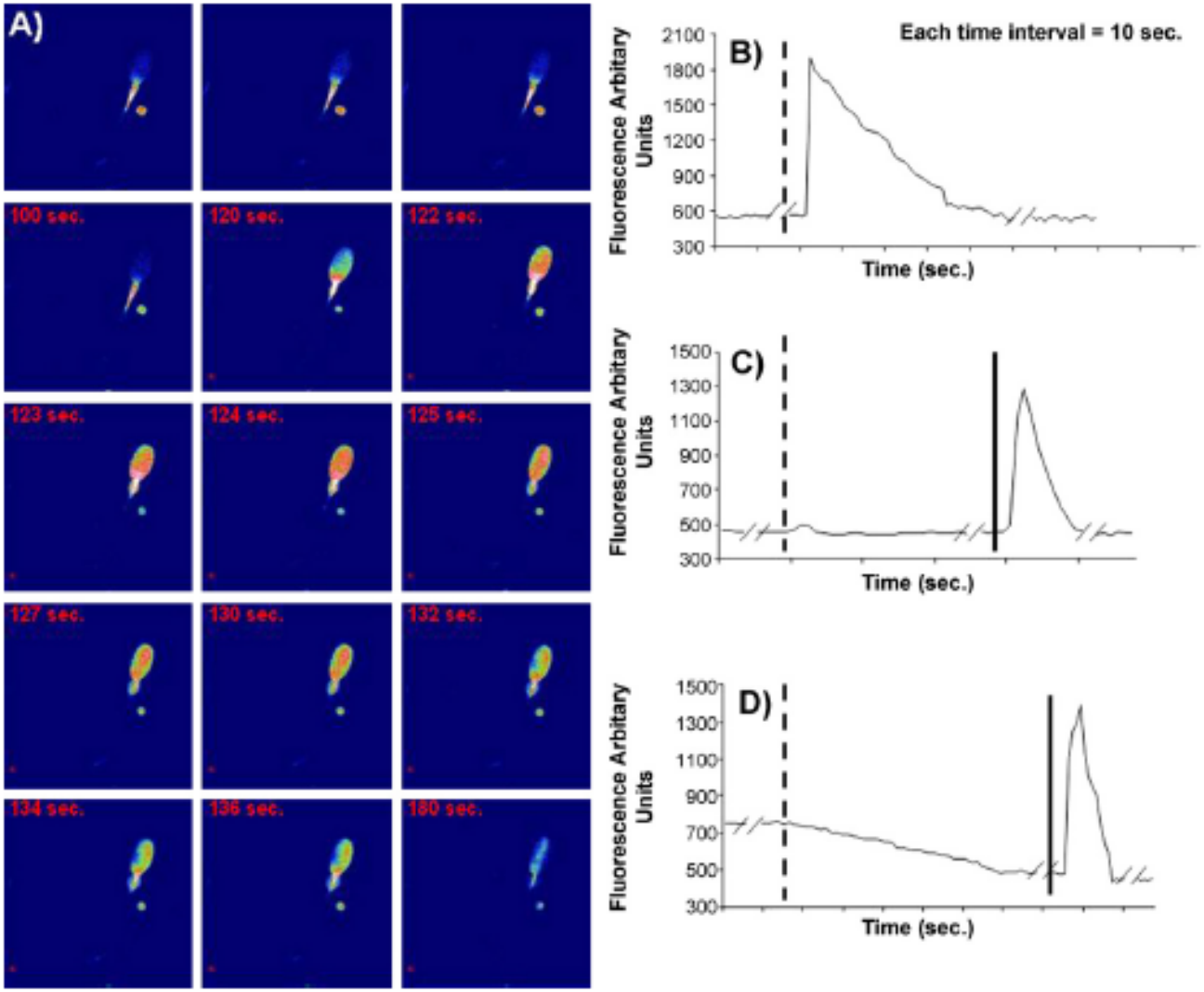

Fig. 3. (A) Confocal image gallery of Fluo-3AM loaded spermatozoa exposed to CPS (asterisk). (B) Effect of CPS (vertical black line) on $[Ca^{2+}]_i$ of one spermatozoa recorded in control cultural condition. Notice that the rise in the $[Ca^{2+}]_i$ in spermatozoon is evident after <10 s from CPS addition, whereas return on the baseline occurs after <40 s. (C) Effect of CPS (vertical black line) on $[Ca^{2+}]_i$ of one spermatozoa recorded in choline chloride medium. In order to investigate the ion mechanism involved in the influence of CPS on intracellular Ca^+ rise, the spermatozoa are recorded in Na^+ free medium. The absence of Na^+ from extracellular environment prevents the rise in $[Ca^{2+}]_i$ induces by CPS while ionomycin added at the end of recording interval promptly induced a rise in $[Ca^{2+}]_i$. (D) Effect of CPZ (vertical dot black line) on $[Ca^{2+}]_i$ of one spermatozoa recorded in control cultural condition The vertical black line correspond to the final addition of ionomycin.

TRPV1

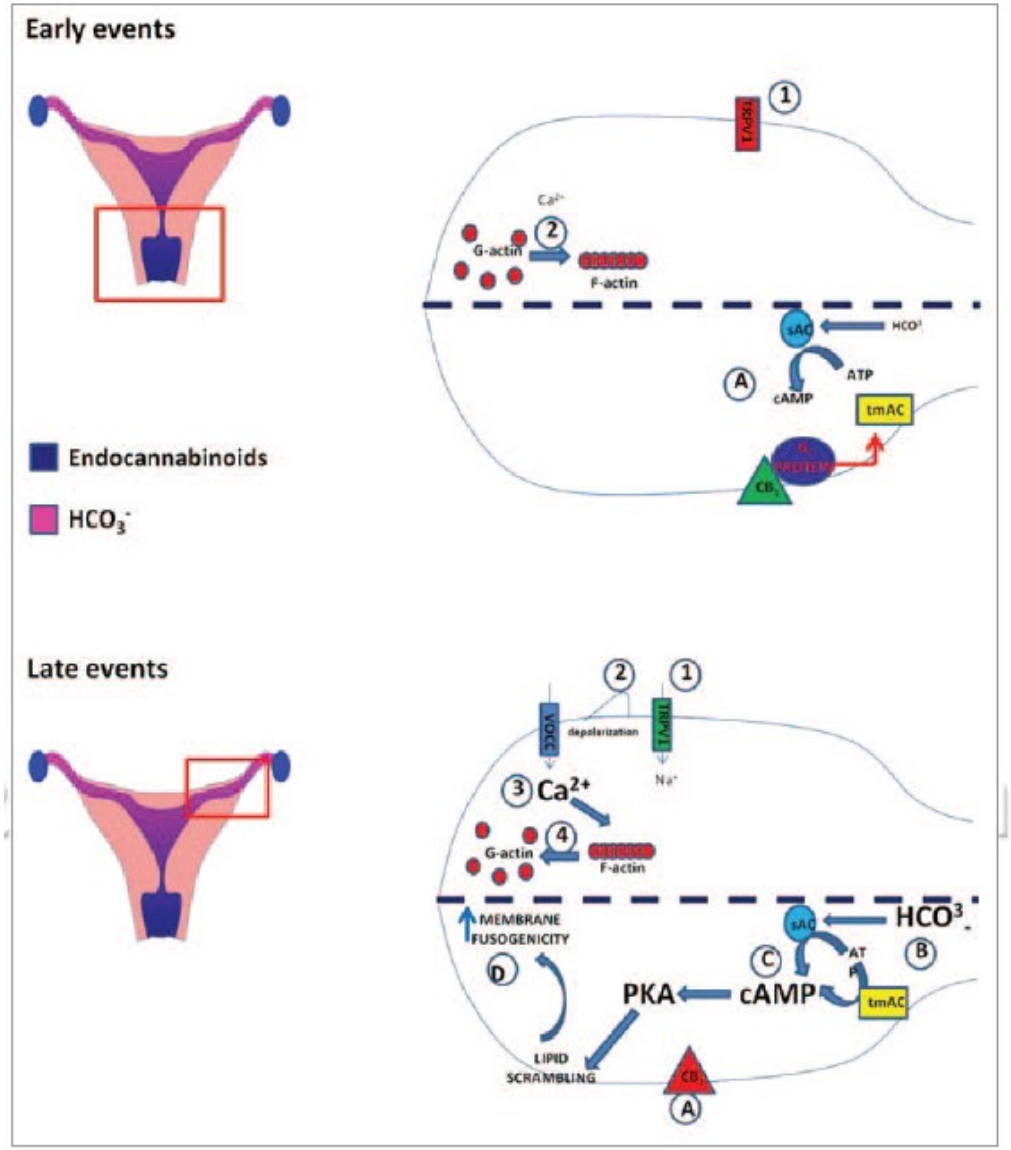
Early events
Endocannabinoids
HCO_3^-
TRPV1
1
Ca^{2+}
2
G-actin
F-actin
sAC
HCO^3
A
ATP
cAMP
tmAC
Late events
2
1
VDCC
depolarization
TRPV1
Na^+
3 Ca^{2+}
4
G-actin
F-actin
MEMBRANE FUSOGENICITY
D
sAC
HCO^3
C
B
AT
PKA
cAMP
tmAC
LIPID SCRAMBLING
A

CatSper channels

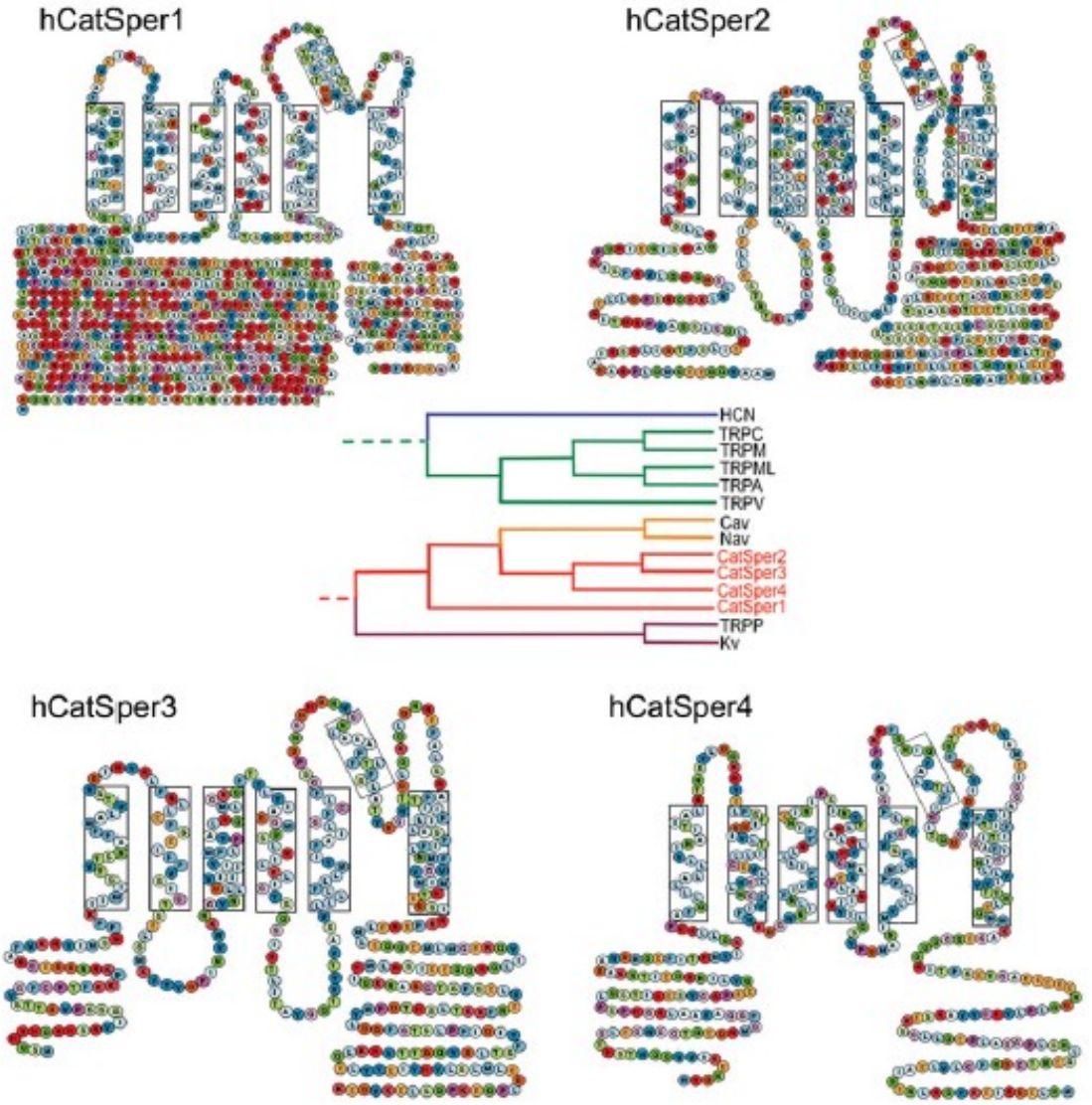

Fig. 1. Human CatSper1-4 predicted secondary topology. *CatSper1-4 have 6TM with a putative voltage sensor (S1-S4) and a pore (S5-S6) domain. Phylogenetic tree (anchored to NaChBac) is shown in the center. Boxes indicate putative transmembrane segments.*

Subunità S1 – S4: sensore di voltaggio

Subunità S5 e6: poro

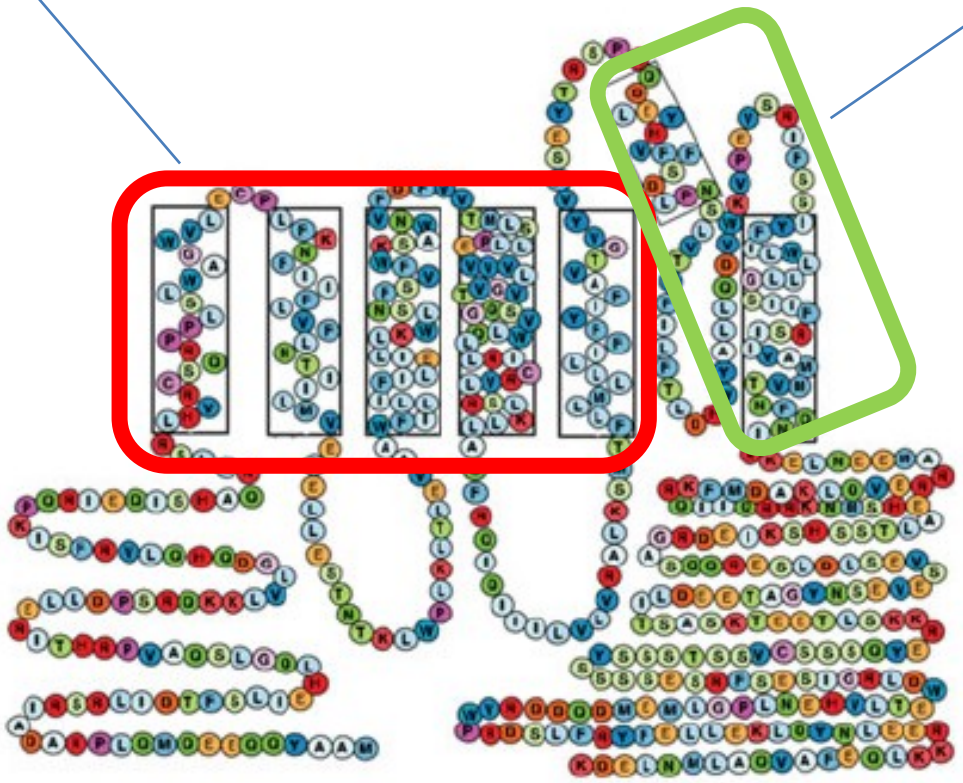

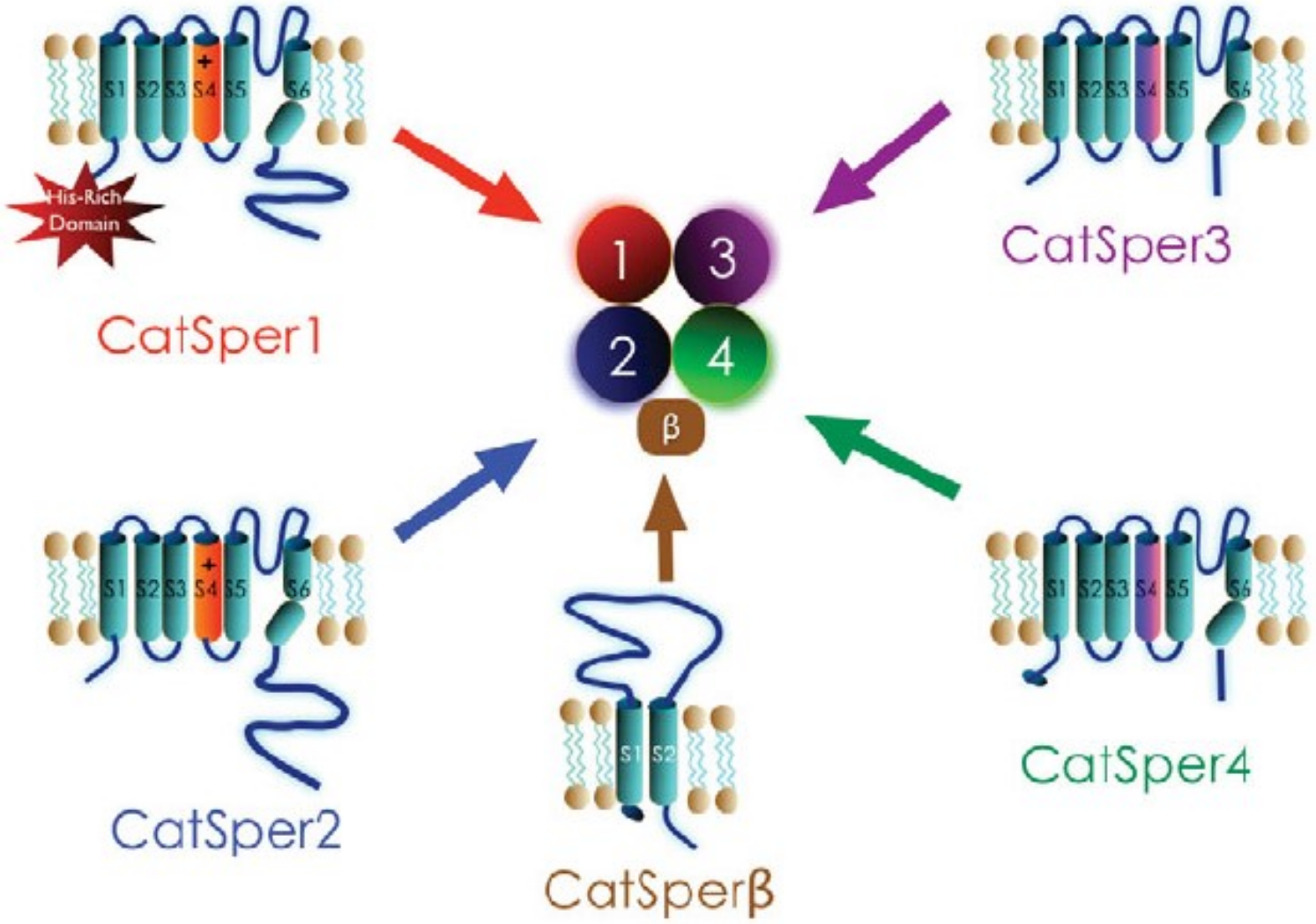

Fig. 2. Heterotetramerization of the CatSper channel. *The CatSper complex is formed from CatSpers1-4 protein subunits and an auxiliary subunit. The CatSper auxiliary subunit, CatSperβ, has 2 predicted transmembrane segments, separated by a large extracellular loop (~1000 amino acids).*

CatSper System

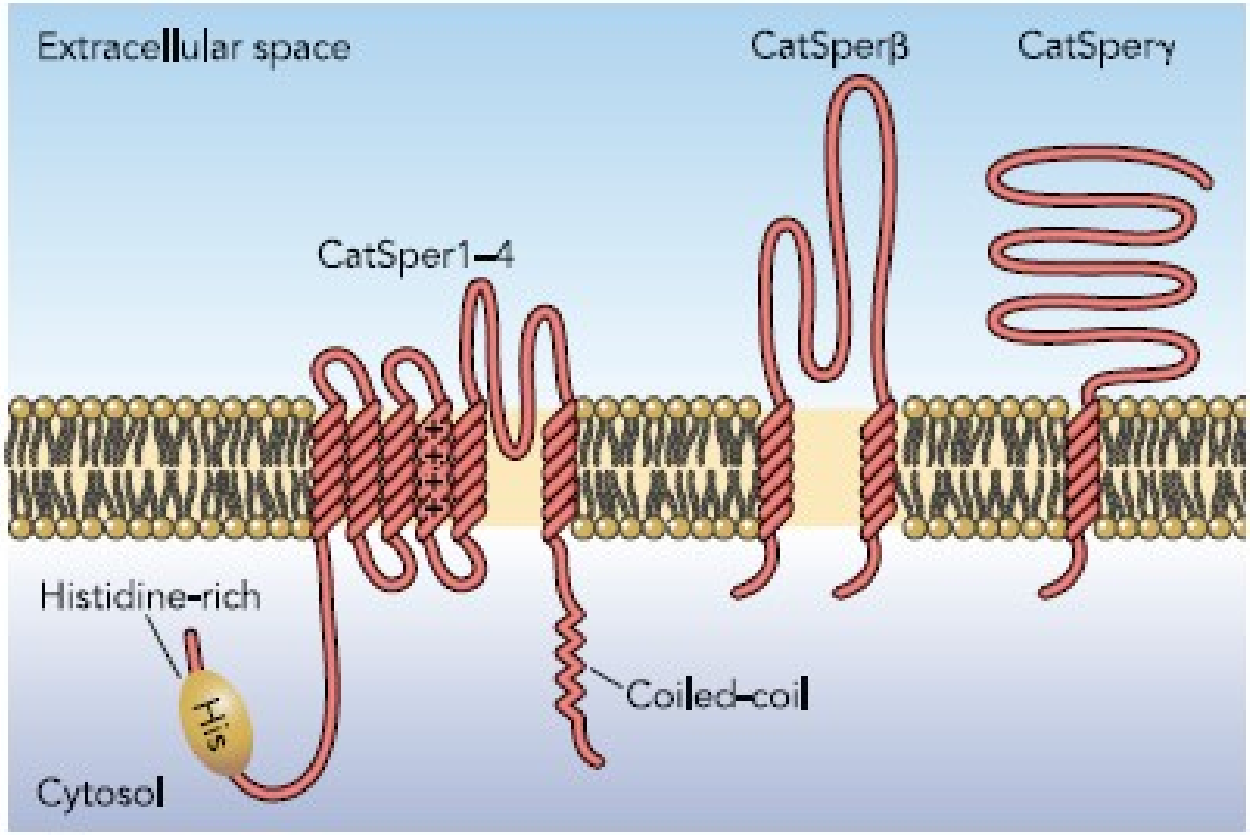

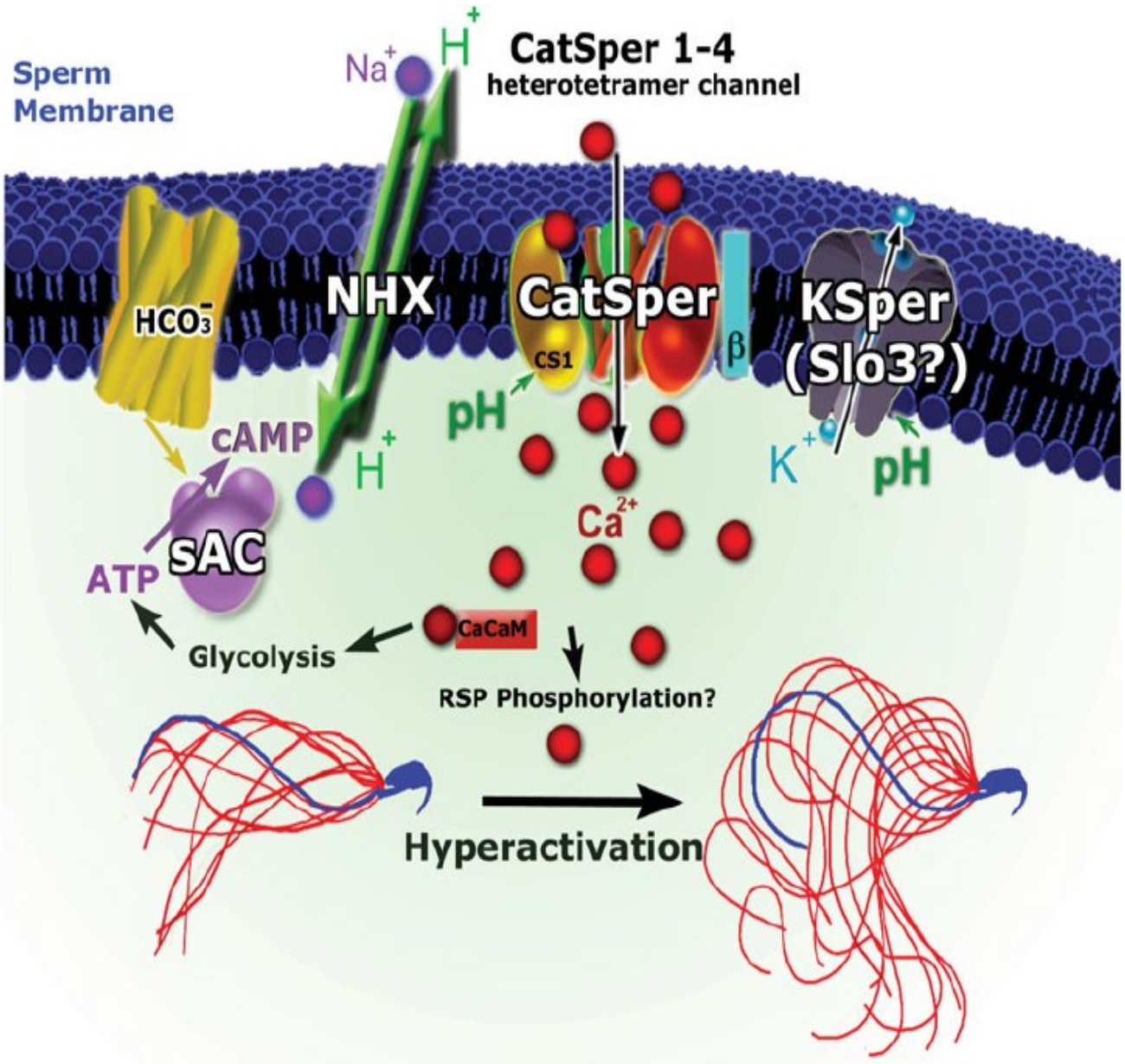

Fig. 3. Spermatozoa ion channel activation and regulation - proposed integrated model. *HCO_3^- ions enter and activate soluble adenylyl cyclase (sAC) that in turn increases cAMP synthesis. cAMP activates (direct or indirectly) the sperm specific Na^+/H^+ exchange (sNHE), thereby increasing intracellular pH. This intracellular alkalinization potently increases $I_{CatSper}$ and I_{KSper}. Alkalinization-mediated potentiation of I_{KSper} hyperpolarizes the membrane potential from ~0 to ~ - 50 mV. Ca^{2+} entry through $I_{CatSper}$ induces a rise in $[Ca^{2+}]_i$, in turn activating Calmodulin (CaCaM) and Calmodulin Kinase (CamK). These changes increase flagellar bending and enhance ATP production, thus increasing sperm endurance and hyperactivating sperm motility. RSP, radical spoke protein. Images of normal and hyperactivated motile sperm modified after Carlson* et al., *2005.*

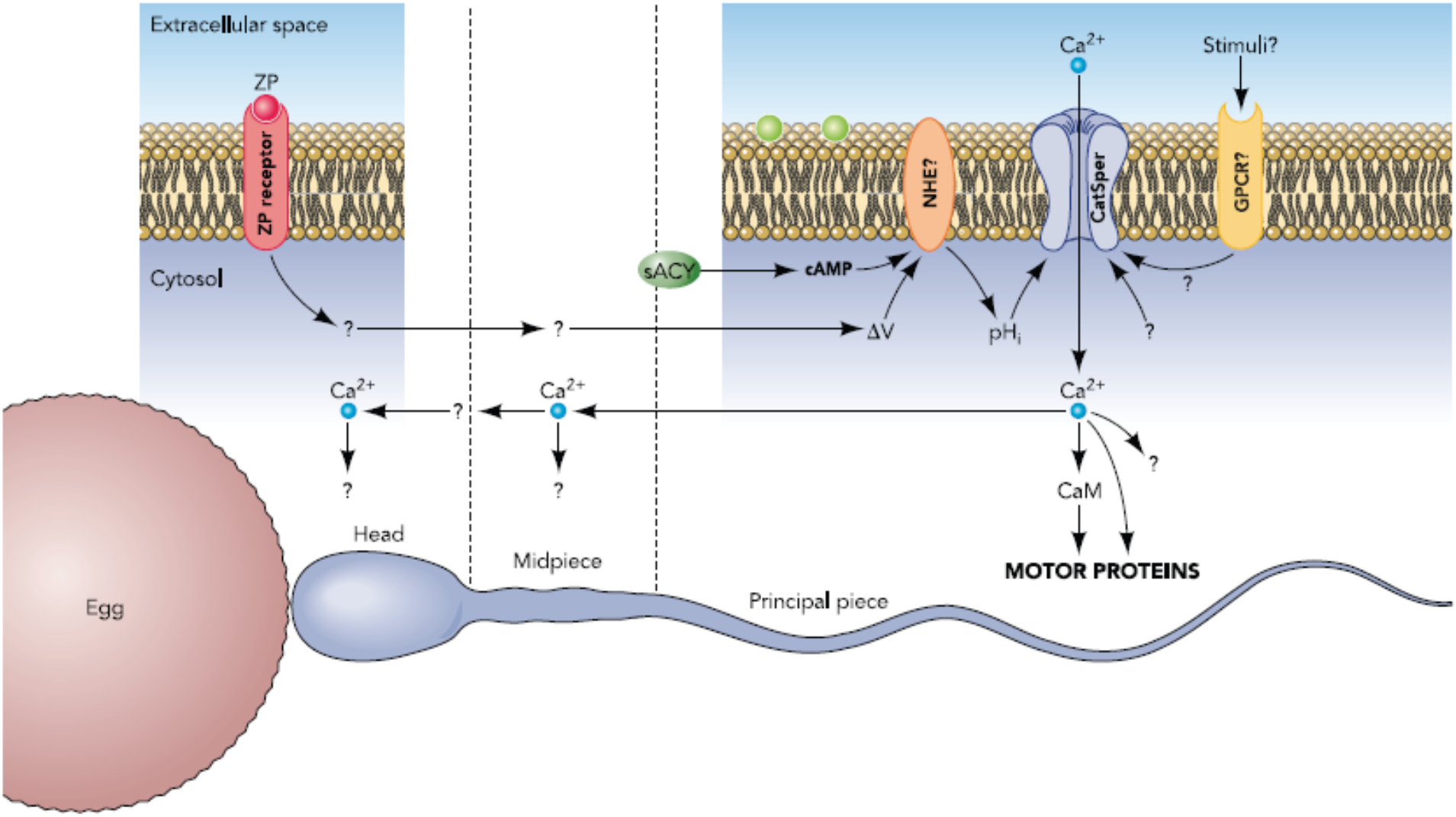

FIGURE 3. **Model for CatSper channel signaling**
In sperm tail, CatSper is activated through alkalinization and perhaps other activators. Intracellular alkalinization can be potentially achieved through a Na^+/H^+ exchanger (NHE) that might be sensitive to cAMP [downstream of a soluble cyclic adenylyl cyclase (sACY)] and voltage. Activation of receptors (e.g., ZP receptors in sperm head) generates messengers that eventually lead to CatSper channel activation in the tail. Ca^{2+} ions entering the sperm tail through CatSper act not only locally on motor proteins to affect sperm motility but also globally to lead to $[Ca^{2+}]_i$ increases in sperm midpiece and head. There are likely unidentified Ca^{2+}-permeable channels responsible for the CatSper-independent, sustained $[Ca^{2+}]_i$ increases important for the acrosome reaction. Many of the proposed signaling pathways have not been directly tested and are indicated by question marks.

CatSper channels

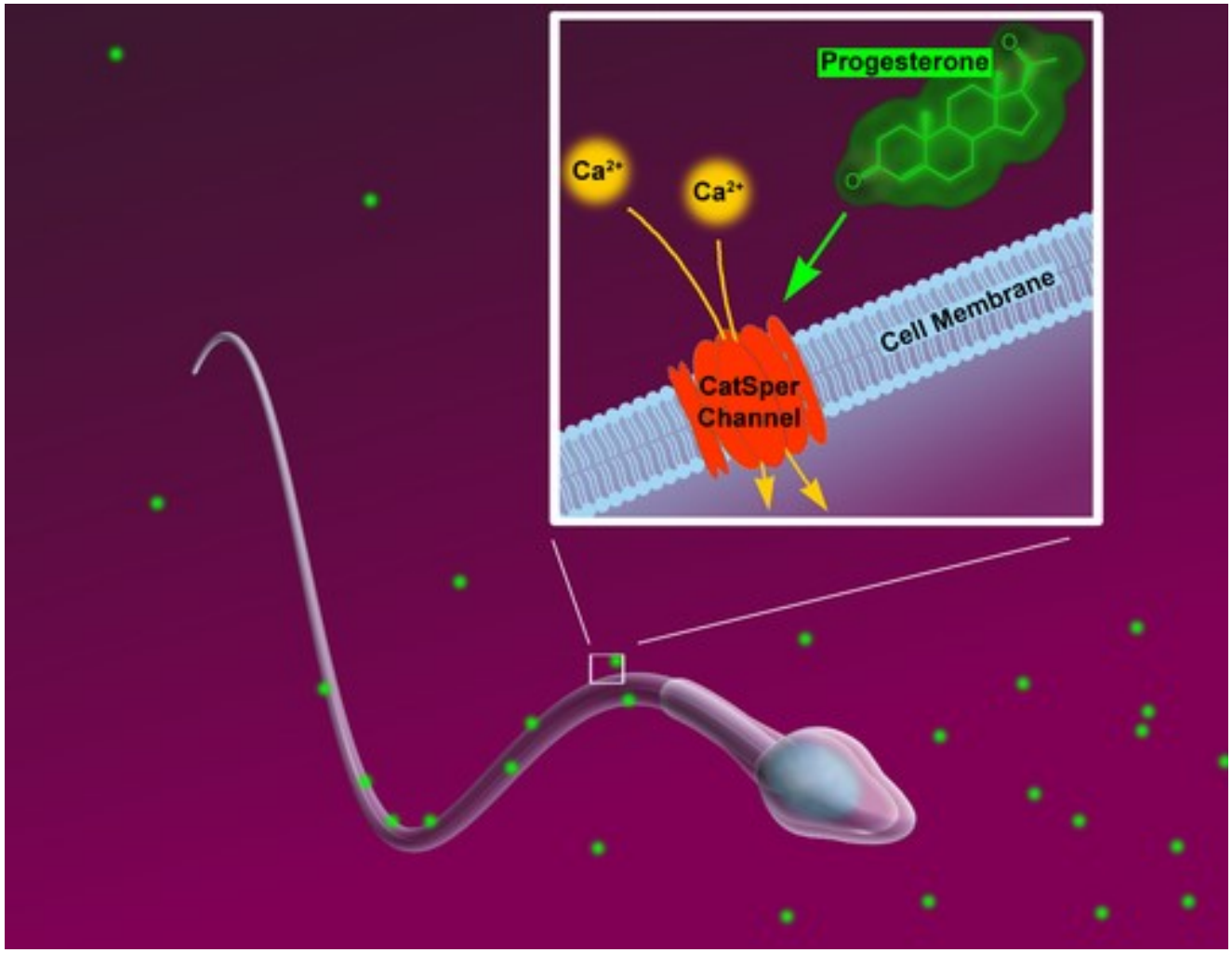

Intracelluar channels

- **IP3R**
- **RyRs**
- **TPCs (Two Pore Channels)**

Motility/Hyperactivation

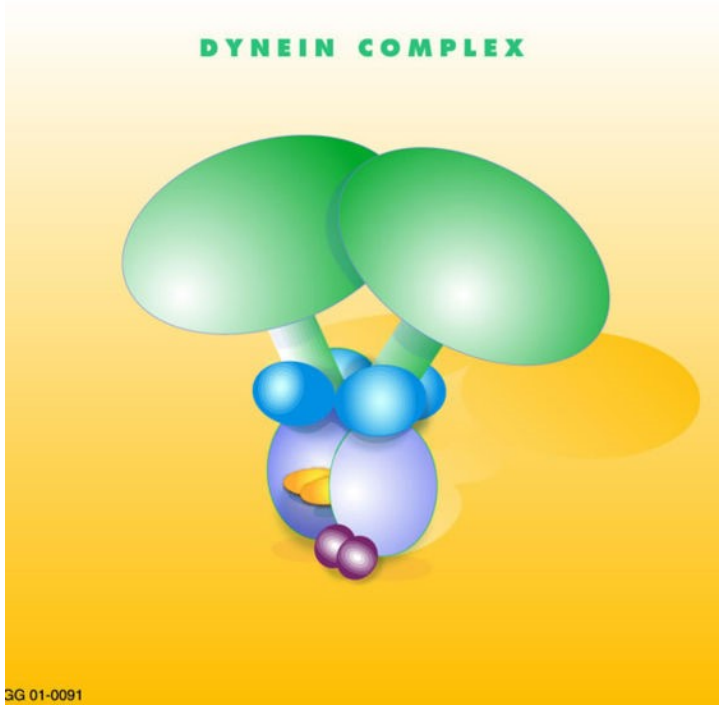

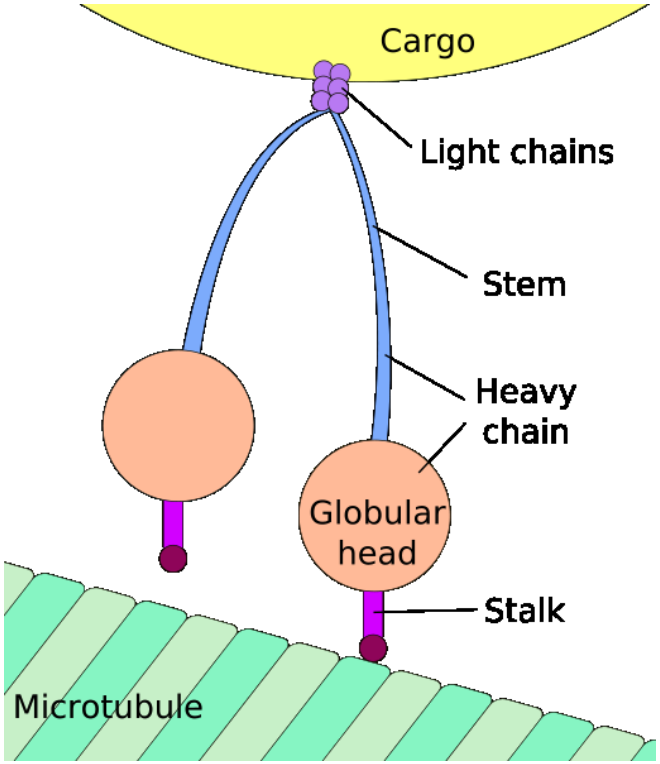

Motility/Hyperactivation

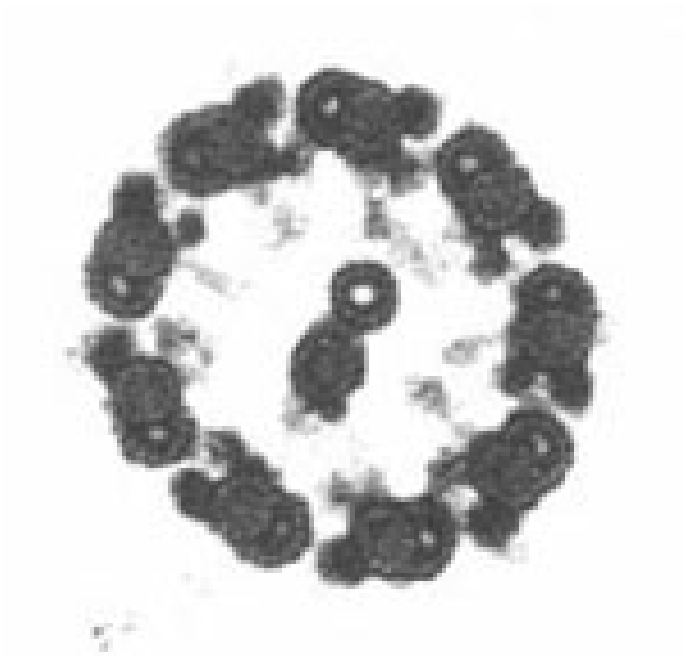

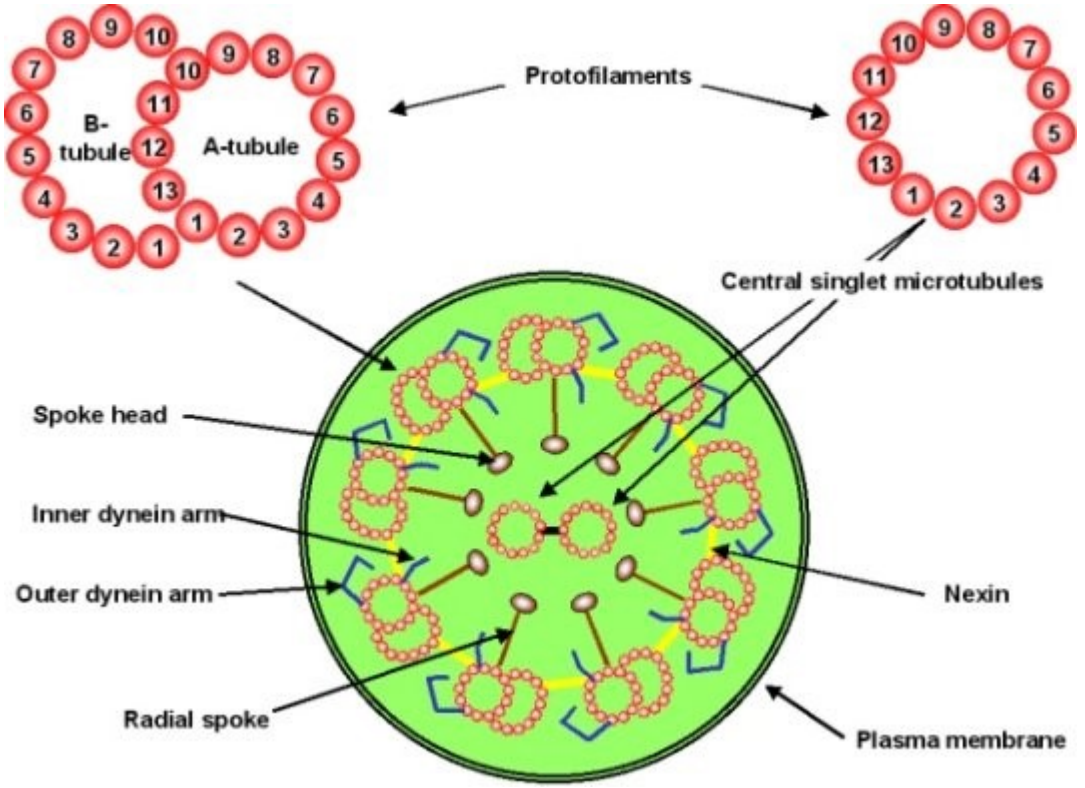

Motility/Hyperactivation

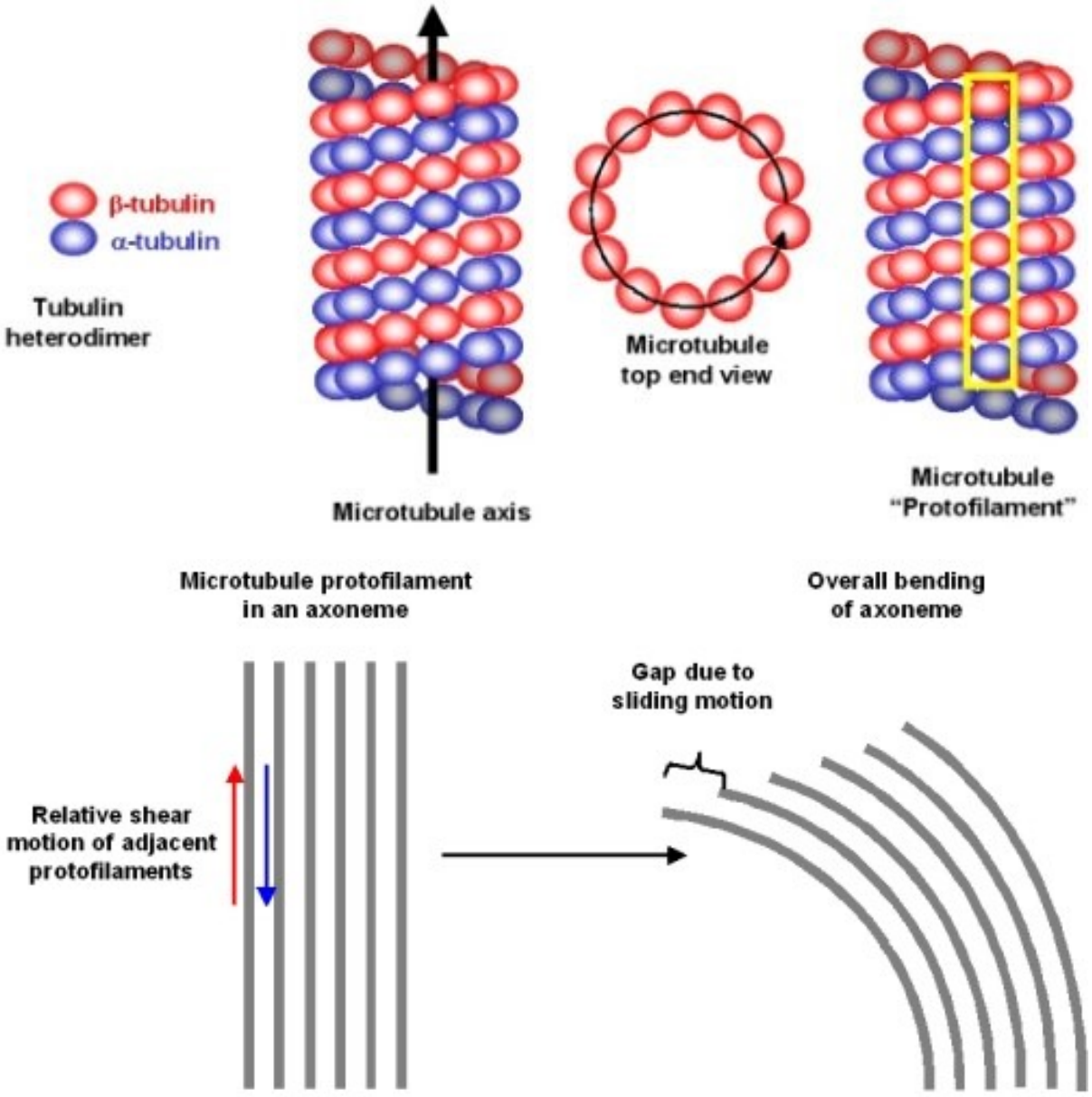

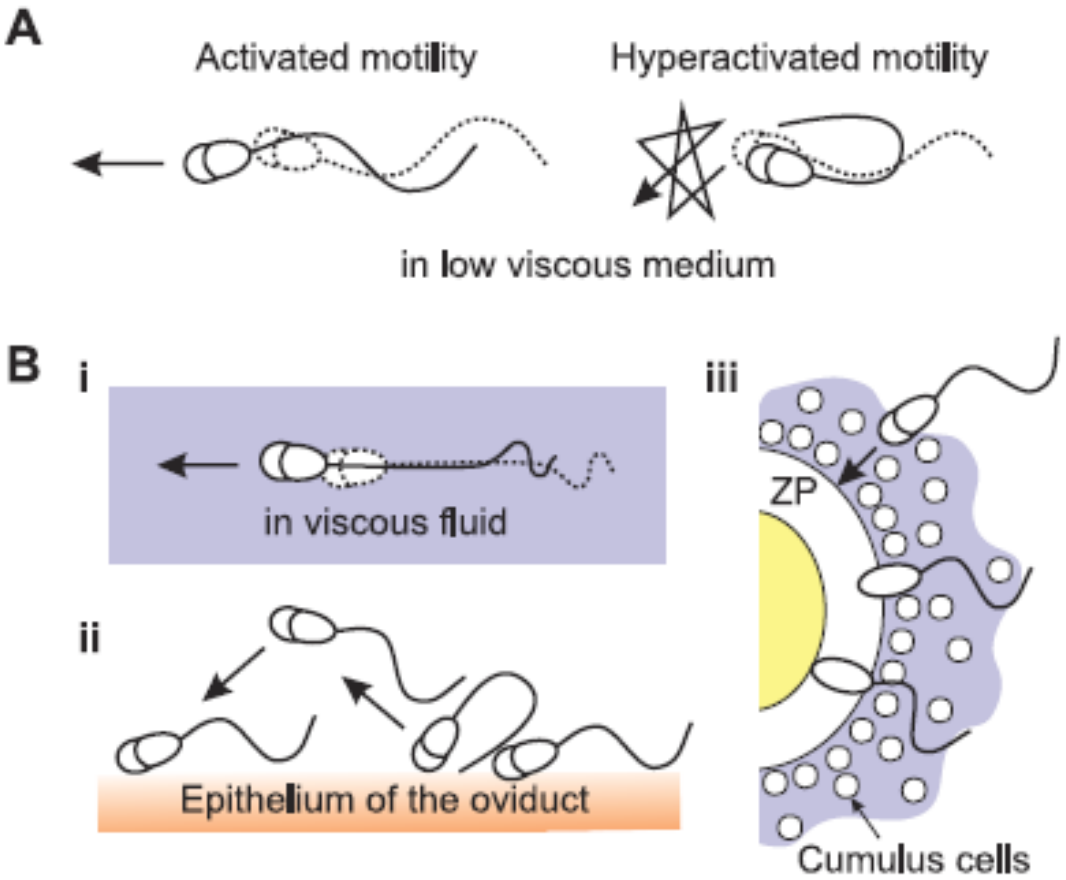

FIGURE 4. Properties and physiological roles of hyperactivation. *A*: activated (*left*) and hyperactivated (*right*) flagellar shape and motility direction (arrows) displayed by spermatozoa in nonviscous experimental media. Activated spermatozoa advance showing a symmetric flagellar bend, while hyperactivated spermatozoa tumble in one place and do not advance efficiently due to an asymmetric flagellar beating pattern. *B*: importance of hyperactivated sperm motility: *i*) To advance in highly viscoelastic fluids in the female genital tract more effectively than activated sperm, *ii*) to detach spermatozoa from the isthmus reservoir and advance towards the ampulla (site of fertilization), and *iii*) to facilitate sperm penetration through the cumulus matrix and the zona pellucida.

Detachment from tubal epithelium

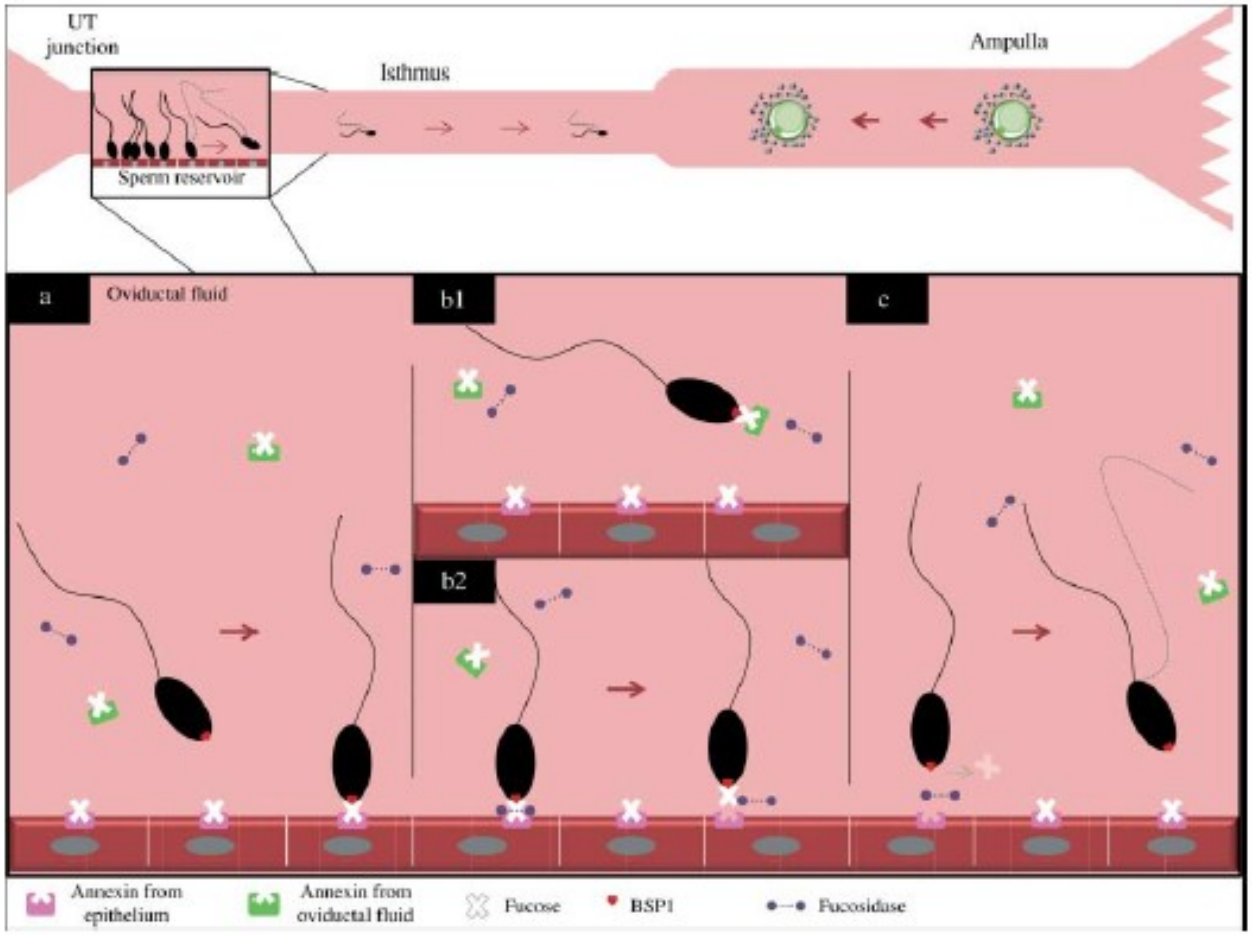

Figure 1 Mechanism for the sperm binding and releasing from the oviduct in the bovine model. (a) Sperm binding is mediated by lectin-like protein as BSP1 present in the sperm plasma membrane that recognizes fucose contained in the annexin molecule bound to the epithelial cell membrane. (b) Sperm binding to the oviduct could be modulated by two different mechanisms that can act at the same time. (b1) Annexin present in the oviductal fluid compete for the BSP1 binding site present on the sperm. (b2) Fucosidase enzymes present in the oviductal fluid can remove fucose residues contained in the annexin present in the oviductal epithelium. (c) These different mechanisms and the development of hyperactivative motility allow the sperm release from the oviductal reservoir.

Cytosckeleton

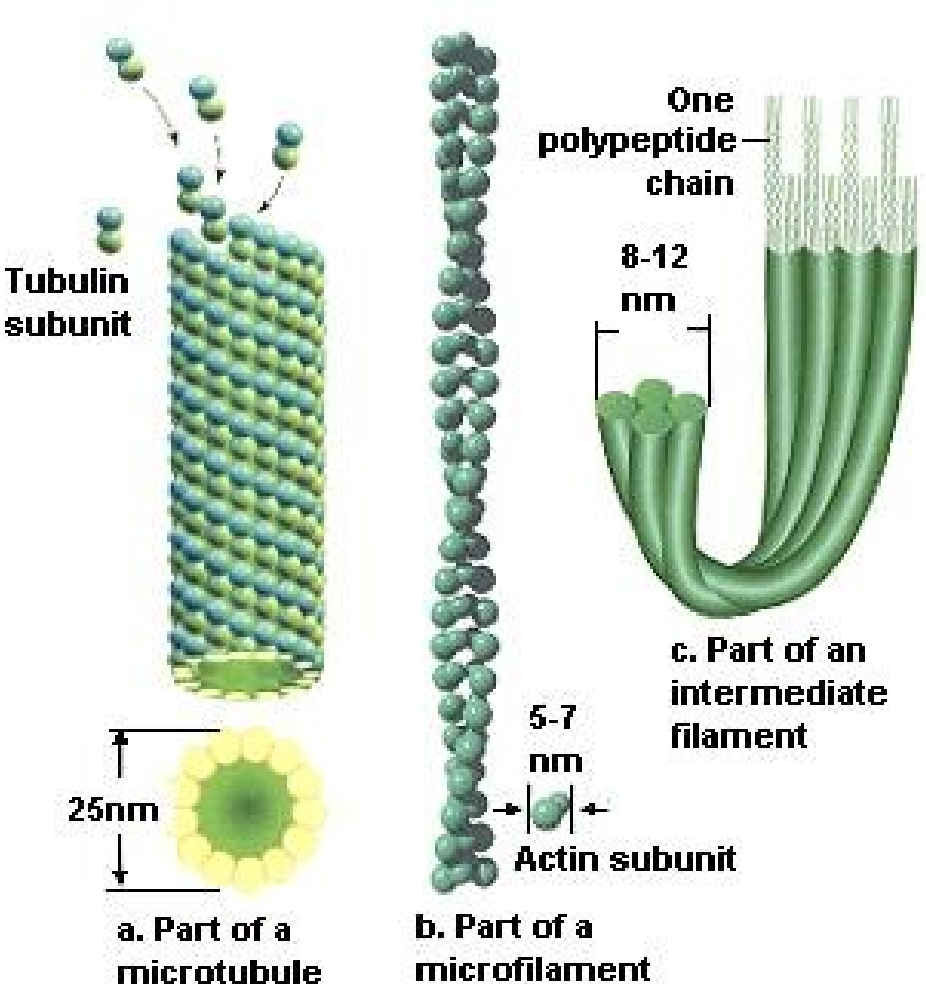

Actin

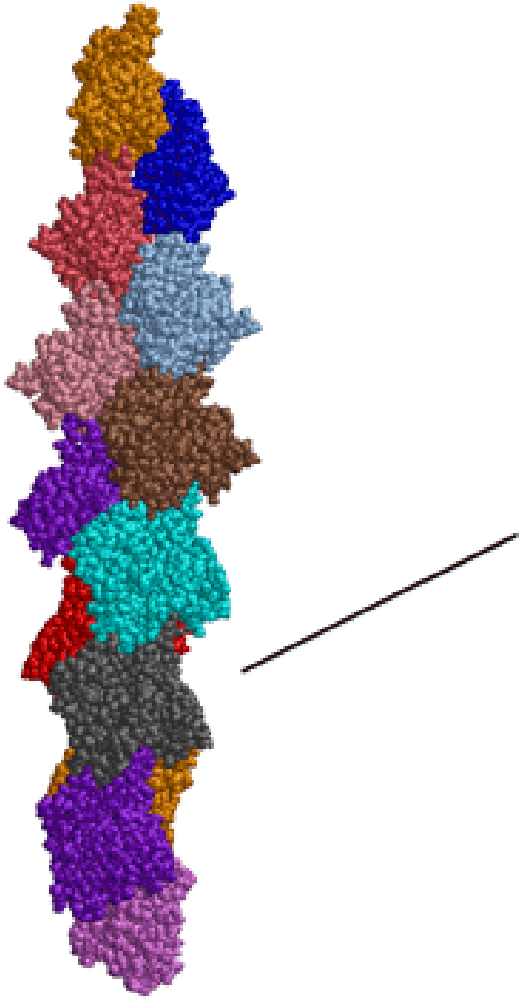

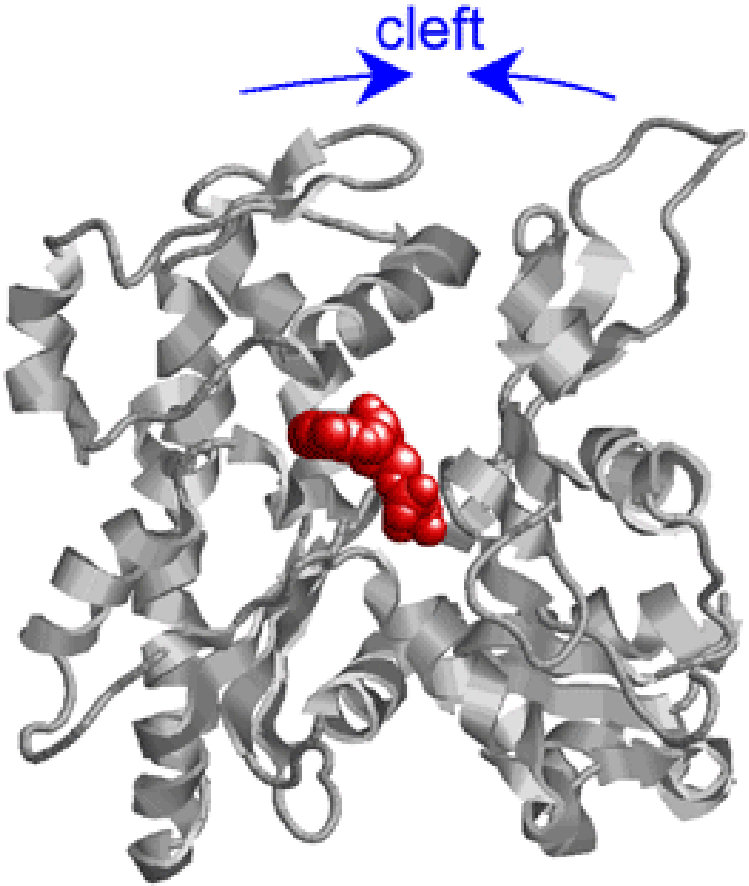

Treadmilling

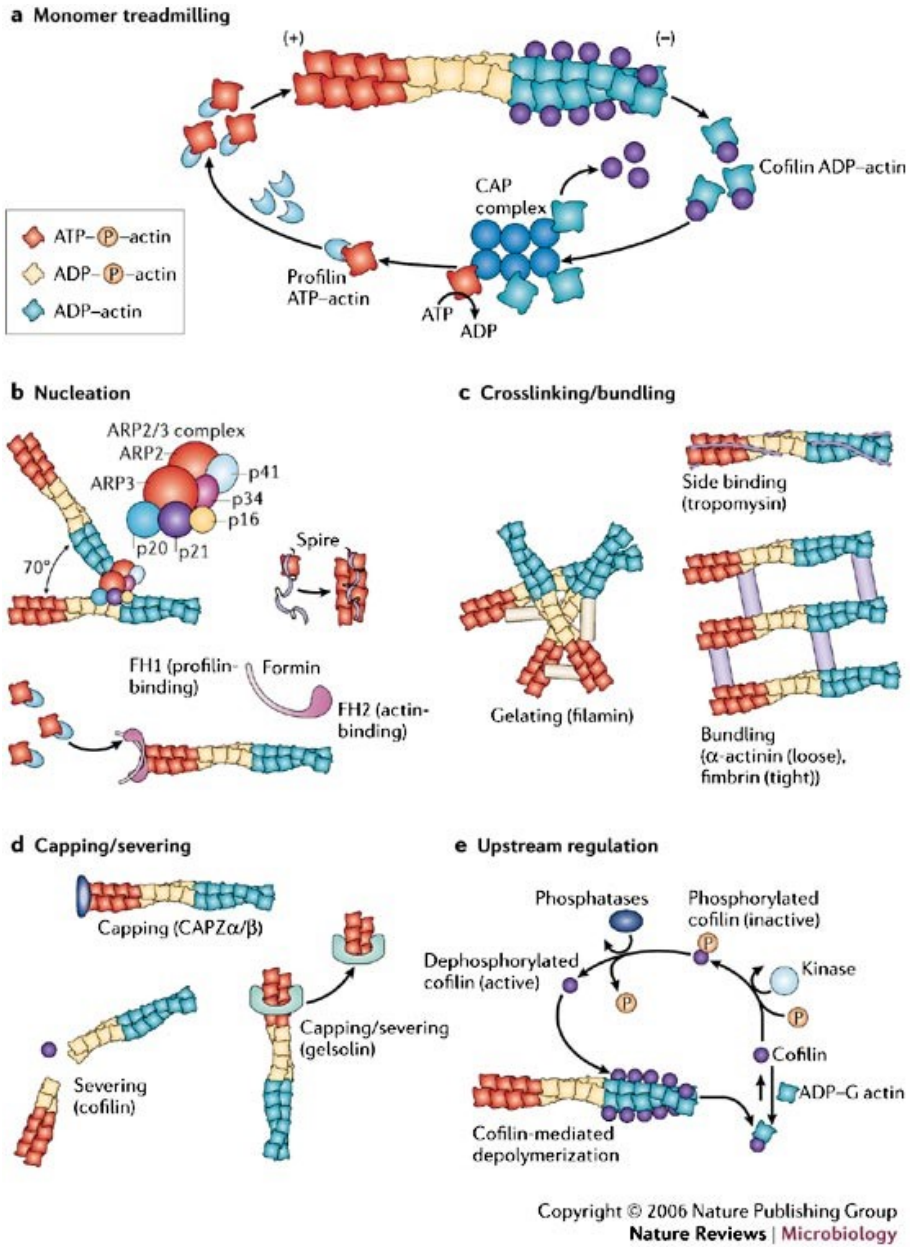

Signal transduction

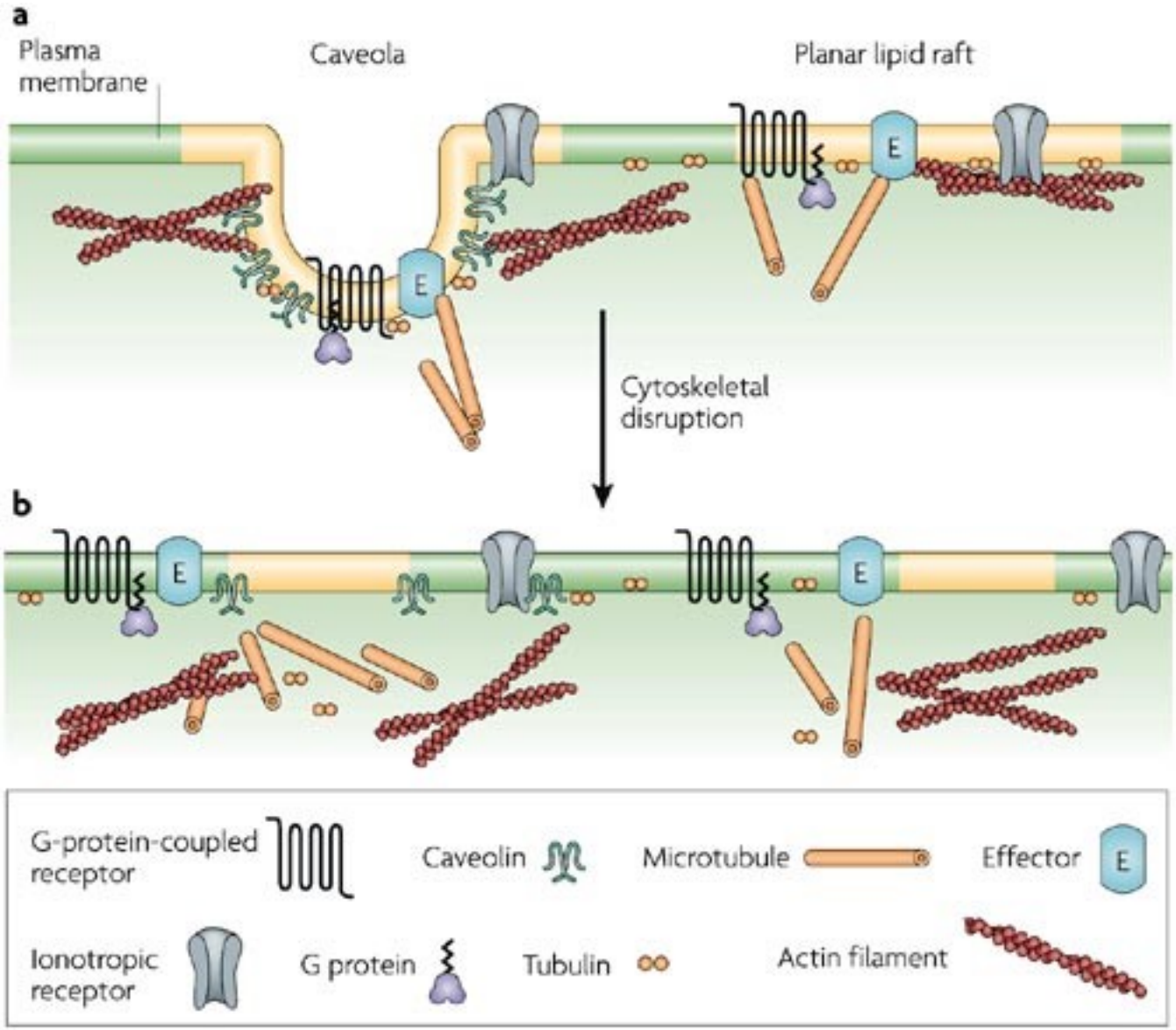

Actin - capacitation

	T_0	Capacitato	Reatto
F-actina	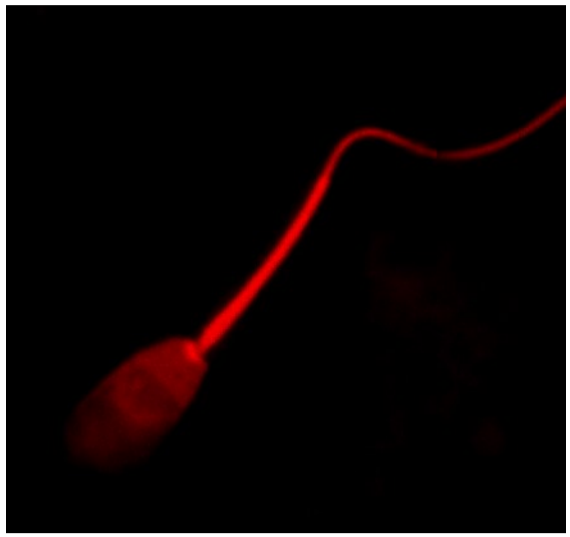	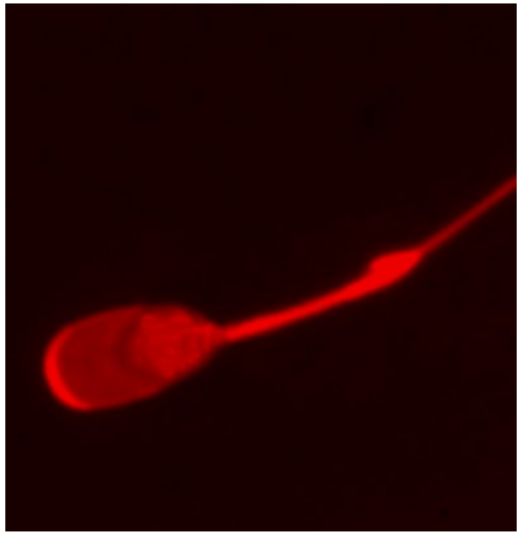	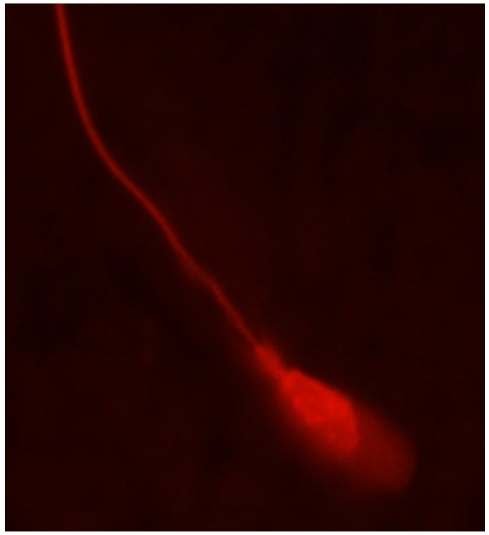

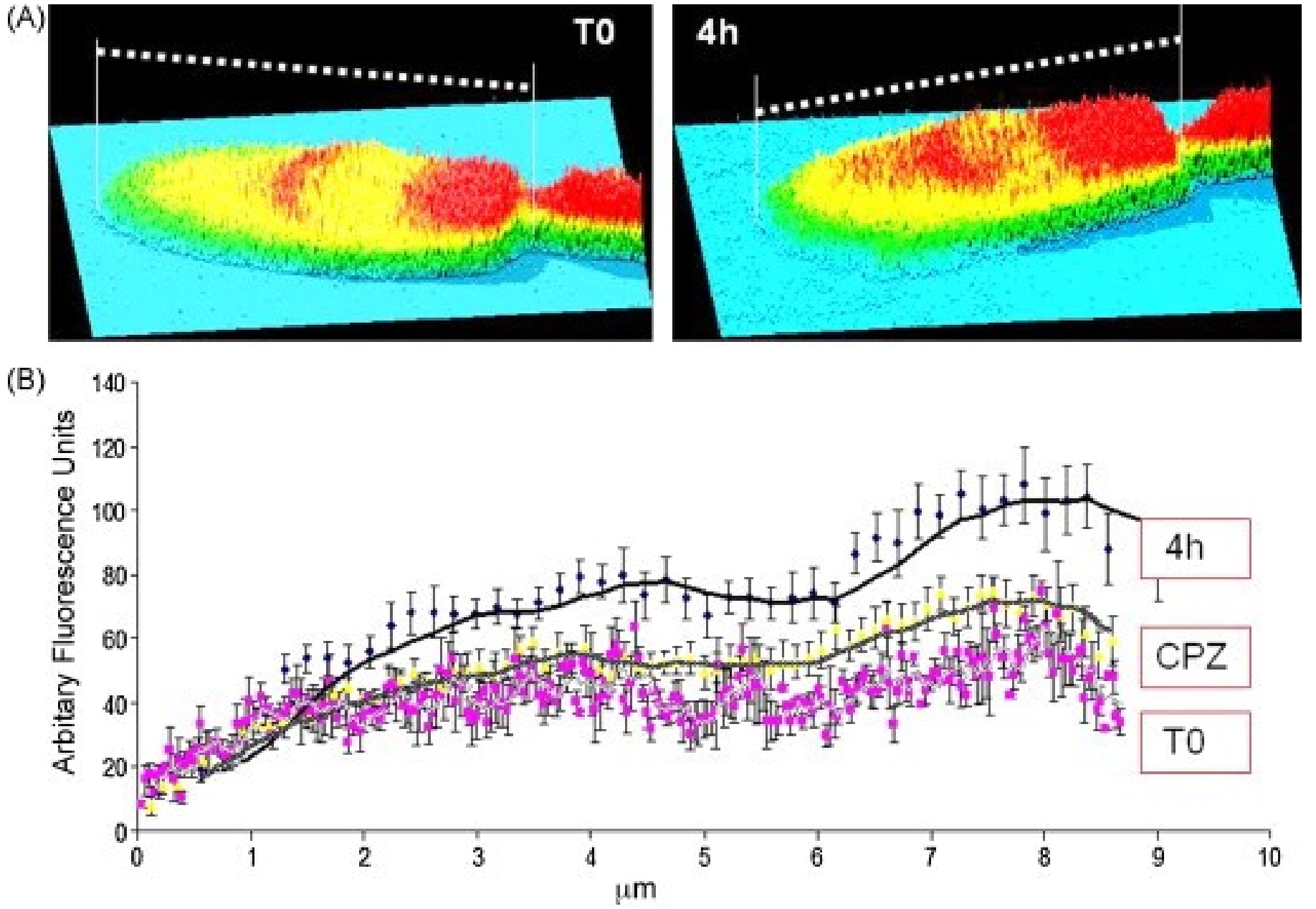
(A)
T0
4h
(B)
Arbitary Fluorescence Units
140
120
100
80
60
40
20
0
0
1
2
3
4
5
6
7
8
9
10
µm
4h
CPZ
T0

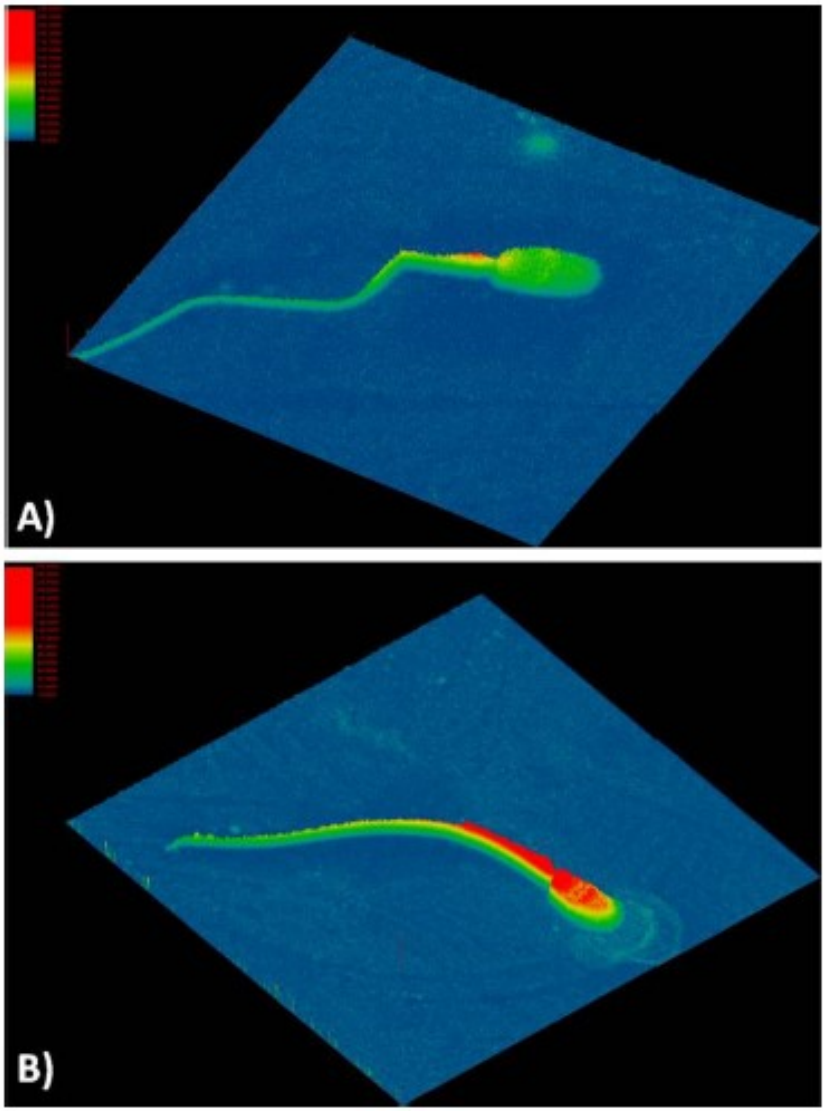

Figure 3 Confocal image representing actin localization in ejaculated and in capacitated spermatozoa. Confocal image representative of TRITC-phalloidin distribution on freshly ejaculated spermatozoon showing a faint fluorescence emission over the midpiece and post-acrosomal region (pattern A; panel A) and of incubated spermatozoon, displaying high fluorescence emission over the whole head (pattern B; panel B).

Protein phosphorylation pattern

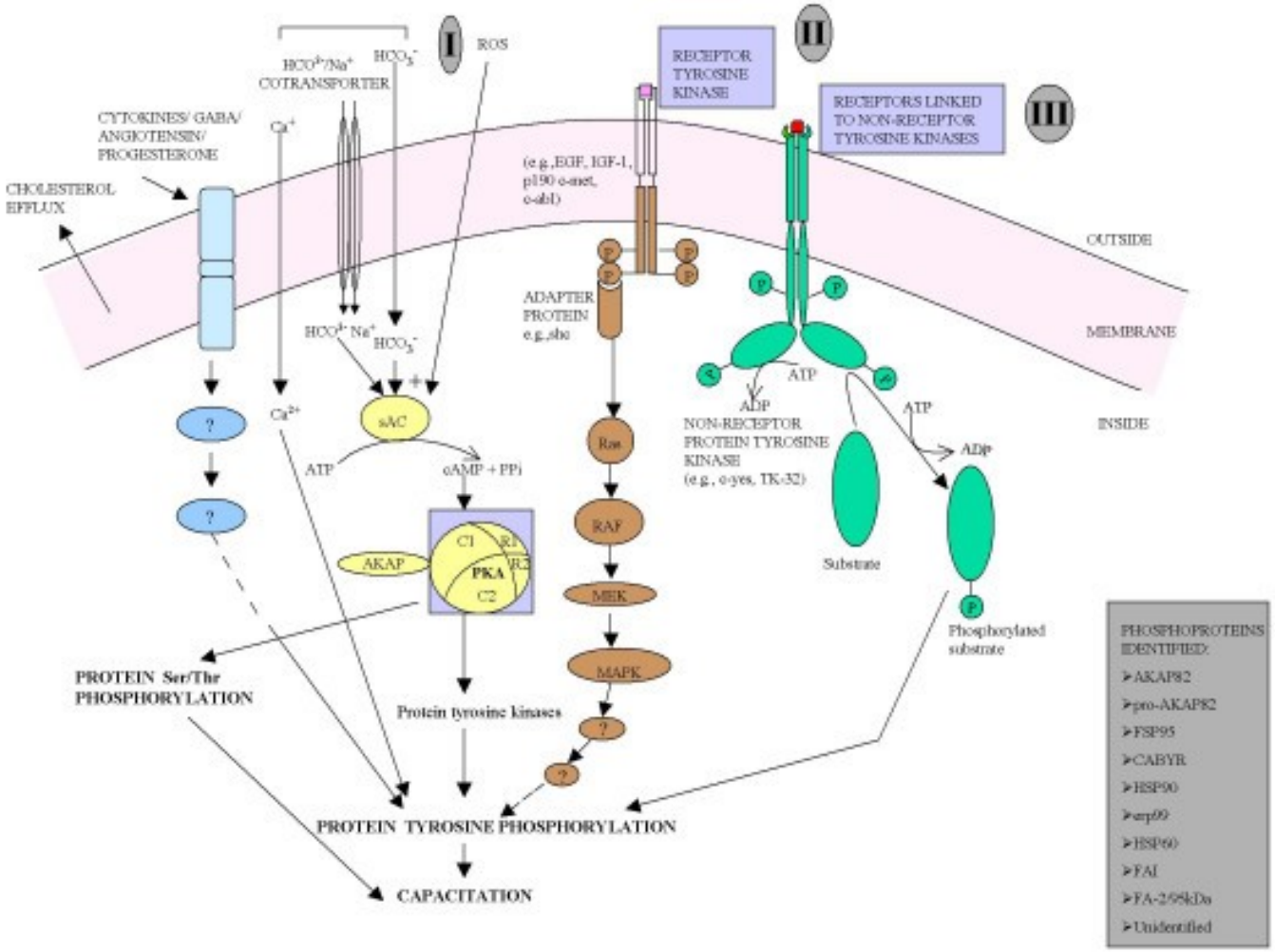

P-Tyr

• tyrosine phosphorylation (capacitation, hyperactivayed motility, ZP binding, sperm-oocyte binding and fusion).

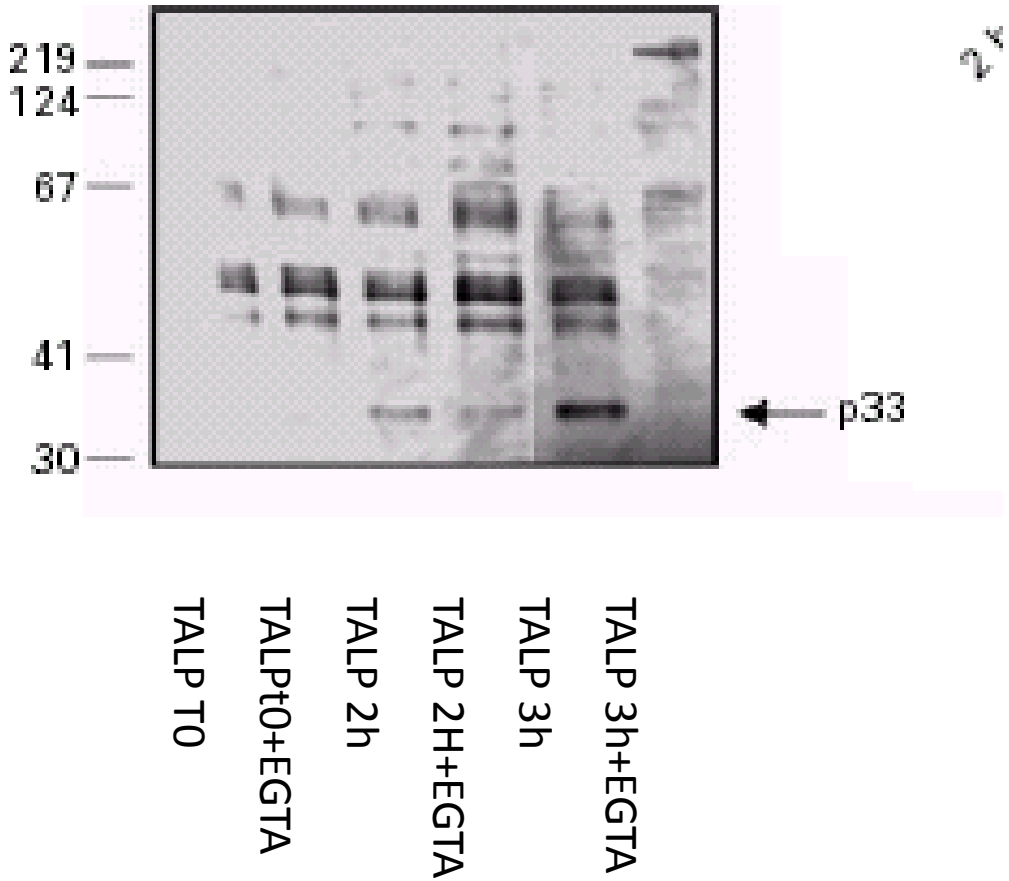

*Green and Watson; Reprodution **122**, 889–898 (2001)*

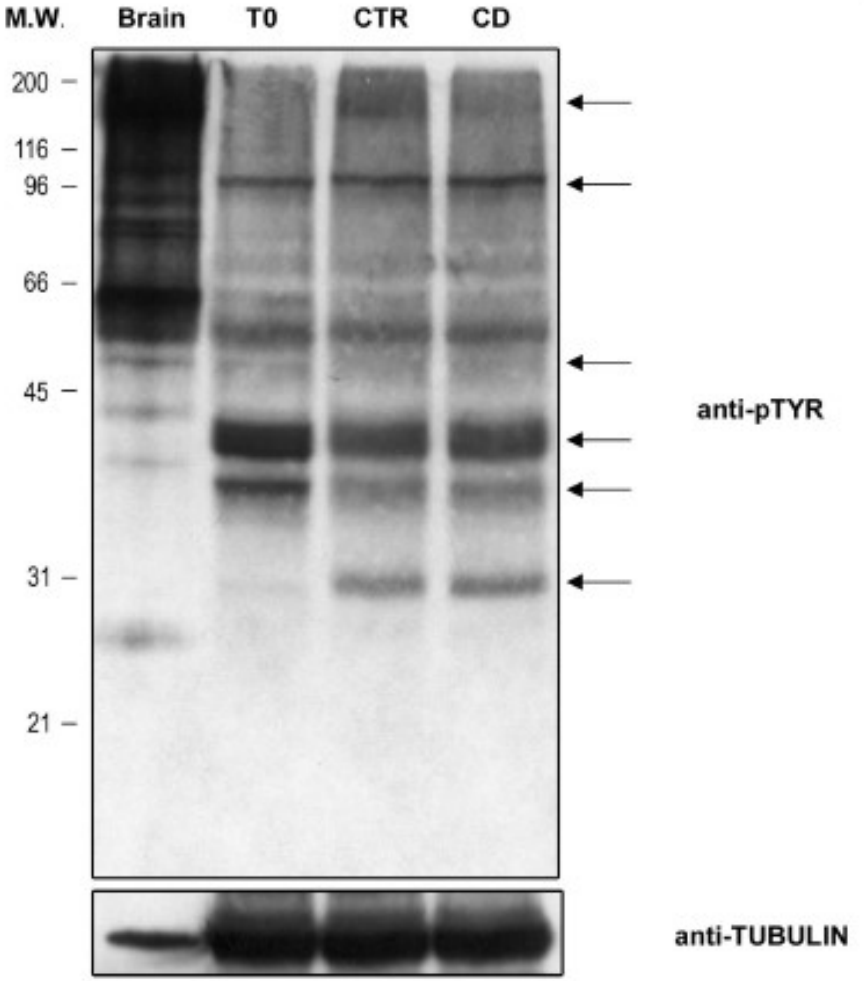

Figure 6 Tyrosine phosphorolation pattern in ejaculated and in capacitated spermatozoa. Western Blot analysis of tyrosine phosphorylation pattern in total lysate of freshly ejaculated male gametes (T0) or in spermatozoa incubated under control condition (CTR) or in the presence of CD (CD). The arrows indicate the capacitation-related changes in P-Tyr. Brain proteins were used as positive control. The filter was normalized on the Tubulin expression. The data shown were representative of three independent experiments.

Nitric oxyde

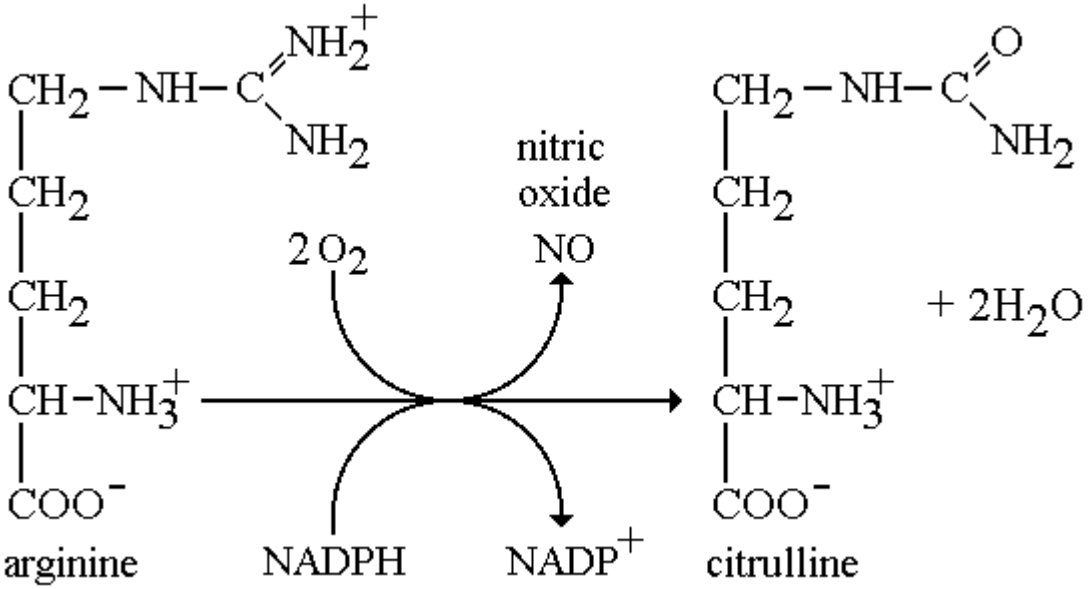

PLCγ1

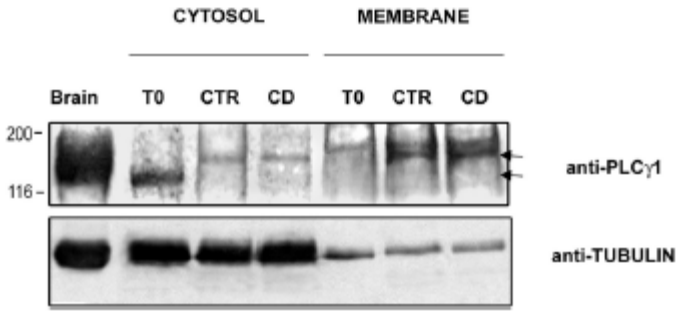

Figure 7 Capacitation-dependent PLCγ1 relocalization. Western Blot analysis of PLCγ1 localization in cytosolic and membrane fractions of freshly ejaculated male gametes (T0) or in spermatozoa incubated under control condition (CTR) or in the presence of CD (CD). The data showing the capacitation-dependent translocation of PLC-γ1 (arrows) from cytosol to membrane. Brain proteins were used as positive control. The filter was normalized on Tubulin expression. The data shown were representative of four independent experiments.

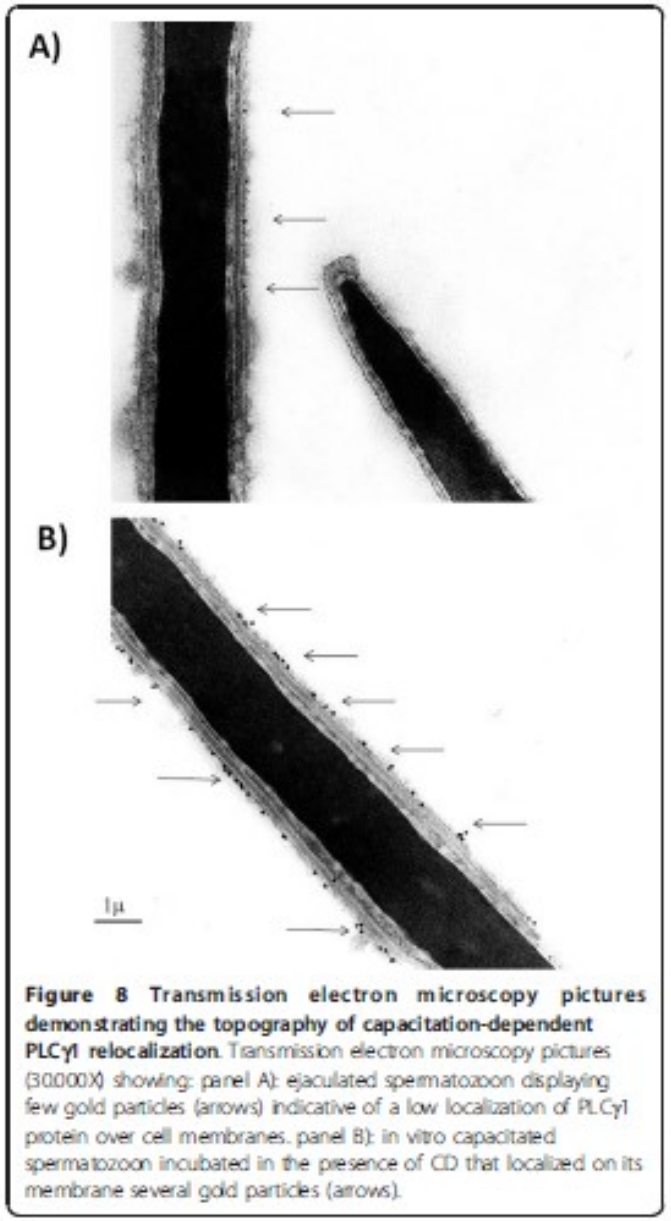

Figure 8 Transmission electron microscopy pictures demonstrating the topography of capacitation-dependent PLCγ1 relocalization. Transmission electron microscopy pictures (30.000X) showing: panel A): ejaculated spermatozoon displaying few gold particles (arrows) indicative of a low localization of PLCγ1 protein over cell membranes. panel B): in vitro capacitated spermatozoon incubated in the presence of CD that localized on its membrane several gold particles (arrows).

Searching for the model…

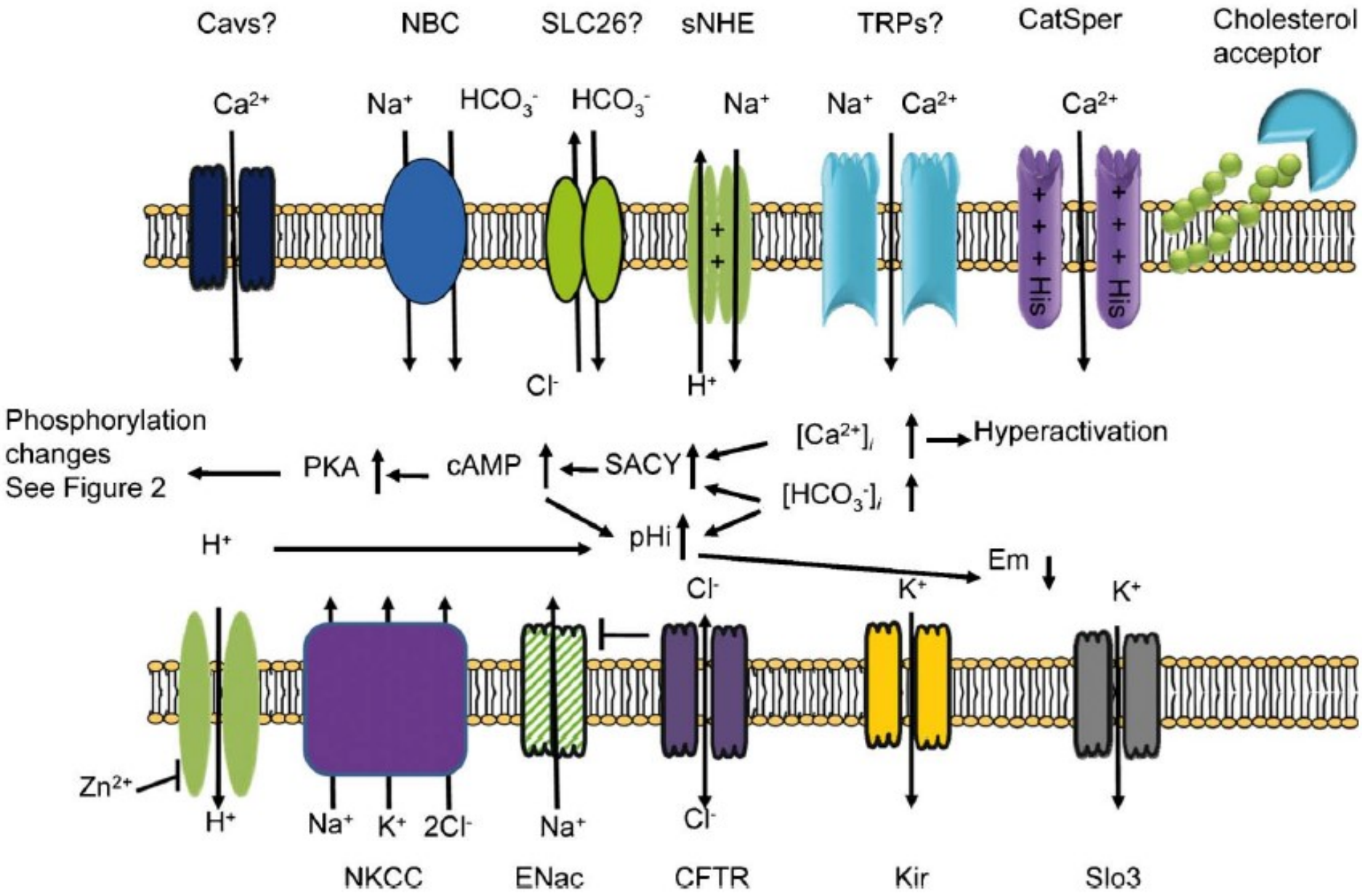

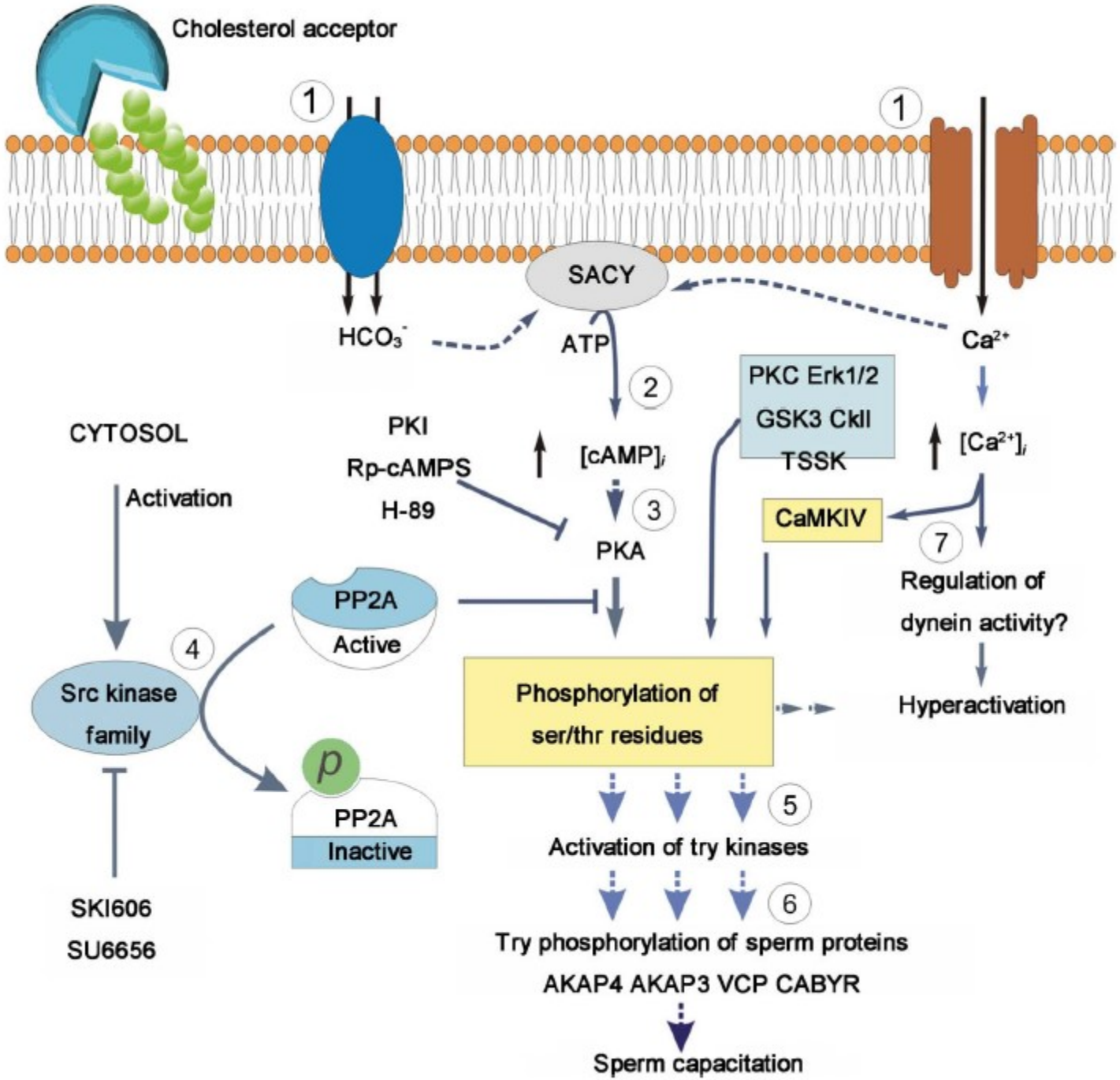
Cholesterol acceptor
1
1
SACY
HCO_3^-
ATP
Ca^{2+}
2
PKC Erk1/2
GSK3 CkII
TSSK
CYTOSOL
PKI
Rp-cAMPS
H-89
$[cAMP]_i$
$[Ca^{2+}]_i$
3
PKA
CaMKIV
7
Regulation of
dynein activity?
Activation
PP2A
Active
4
Src kinase
family
Phosphorylation of
ser/thr residues
Hyperactivation
p
PP2A
Inactive
5
Activation of try kinases
6
Try phosphorylation of sperm proteins
AKAP4 AKAP3 VCP CABYR
SKI606
SU6656
Sperm capacitation

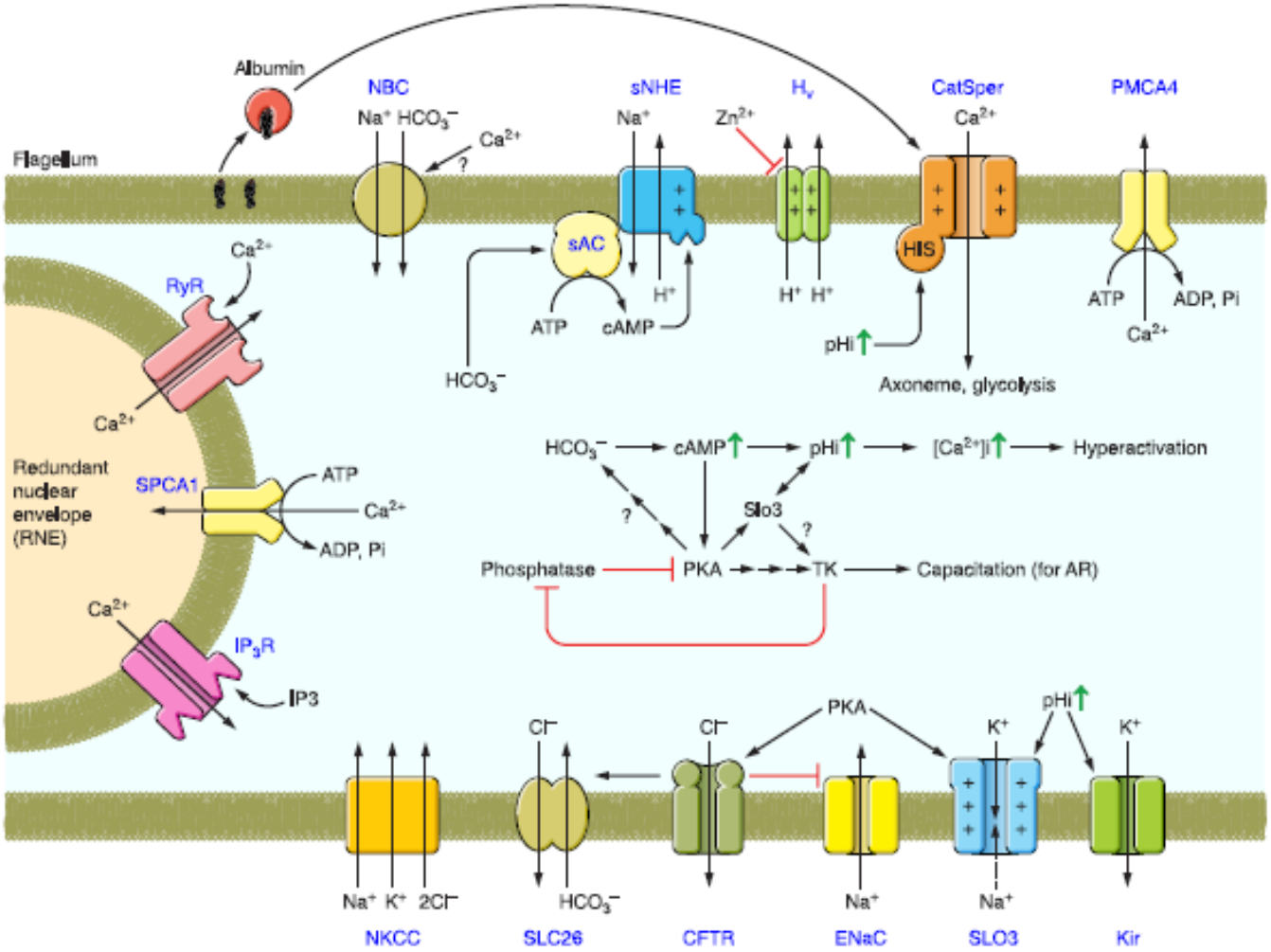

FIGURE 6. Ion fluxes during mammalian sperm hyperactivation and capacitation. Both processes take place during sperm transit through the female tract and have parallel but also intercrossing pathways. Albumin present in the female tract removes cholesterol from the sperm plasma membrane modifying several membrane properties; it may also directly activate CatSper channels, increasing $[Ca^{2+}]_i$. Activation of a Na^+/HCO_3^- (NBC) cotransporter (possibly activated by external Ca^{2+}) increases HCO_3^- levels activating a soluble adenylyl cyclase (sAC) and producing cAMP. This cAMP may activate the sperm Na^+/H^+ exchanger (sNHE) and together with the activation of the proton channel (H_V) (by Zn^{2+} removal) would raise pH_i, another cellular parameter that activates CatSper and SLO3 channels. The overall Ca^{2+} increase may influence glycolysis and the axoneme activity promoting hyperactivation of motility. Several Ca^{2+} mobilizing pumps (PMCA4, SPCA1) and channels [IP_3 receptor (IP_3R), ryanodine receptor (RyR)] may also participate during Ca^{2+} signaling. Concomitantly, the increase in cAMP levels activates PKA, which after several unknown steps stimulates tyrosine kinases to produce the tyrosine phosphorylation associated with capacitation. Possible connections between hyperactivation and capacitation signaling cascades are indicated. In some species, capacitation is accompanied by membrane hyperpolarization; the channels and transporters involved during this process are indicated.

Acrosome reaction

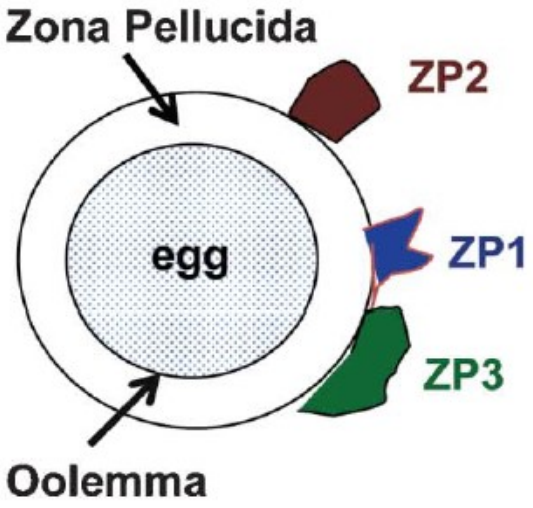

ZP1; ZP2; ZP3

Mouse ZP

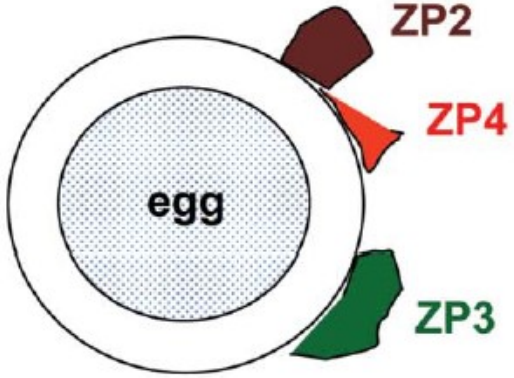

ZP2; ZP3; ZP4

Porcine, bovine and canine ZP

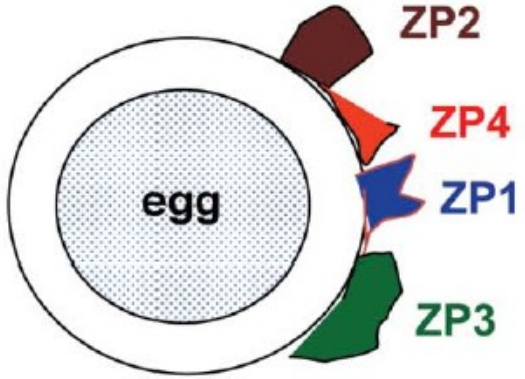

ZP1; ZP2; ZP3; ZP4

Rat, hamster, bonnet monkey and human ZP

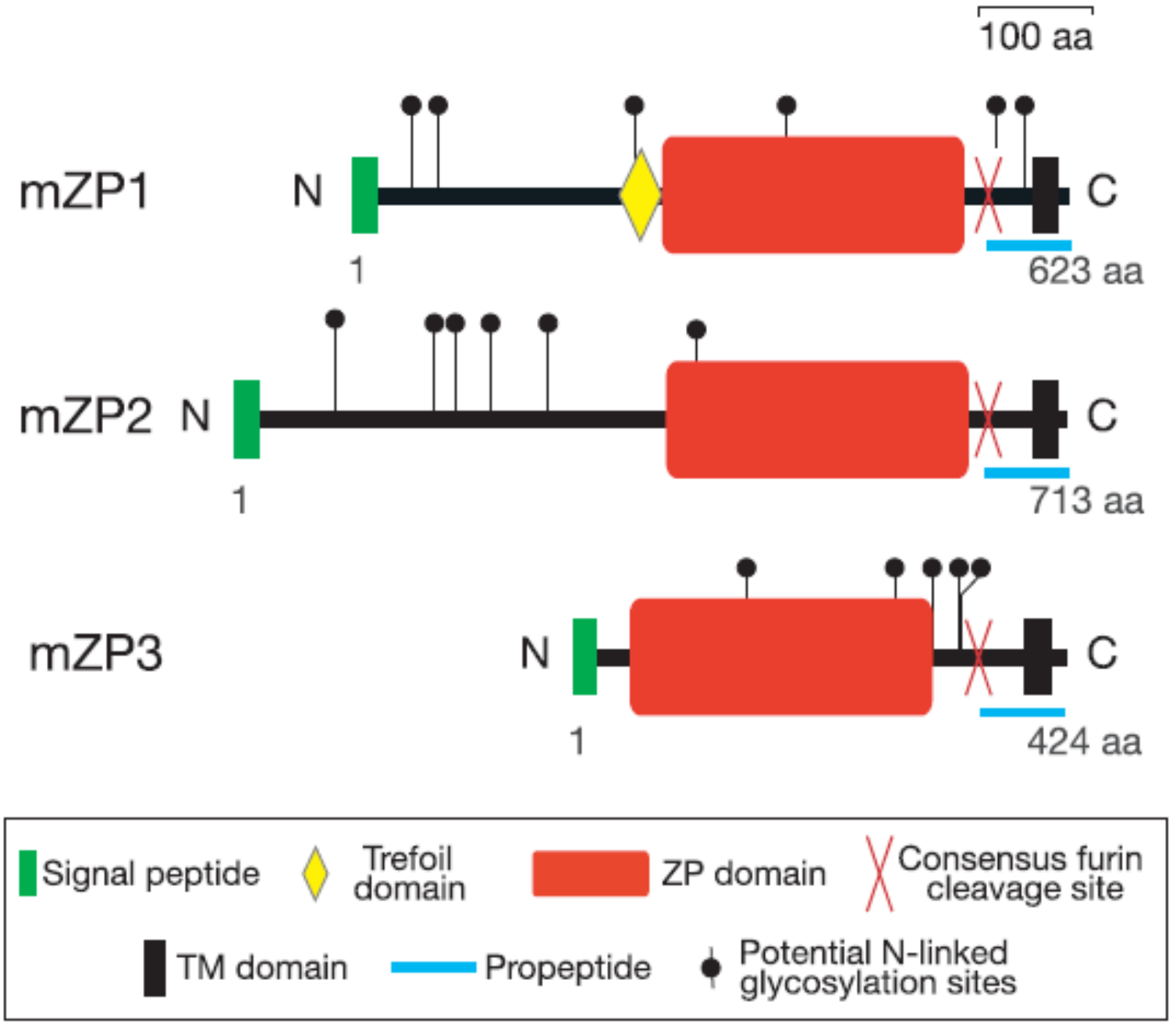
100 aa
mZP1
N
C
1
623 aa
mZP2
N
C
1
713 aa
mZP3
N
C
1
424 aa
Signal peptide
Trefoil domain
ZP domain
Consensus furin cleavage site
TM domain
Propeptide
Potential N-linked glycosylation sites

ZP3

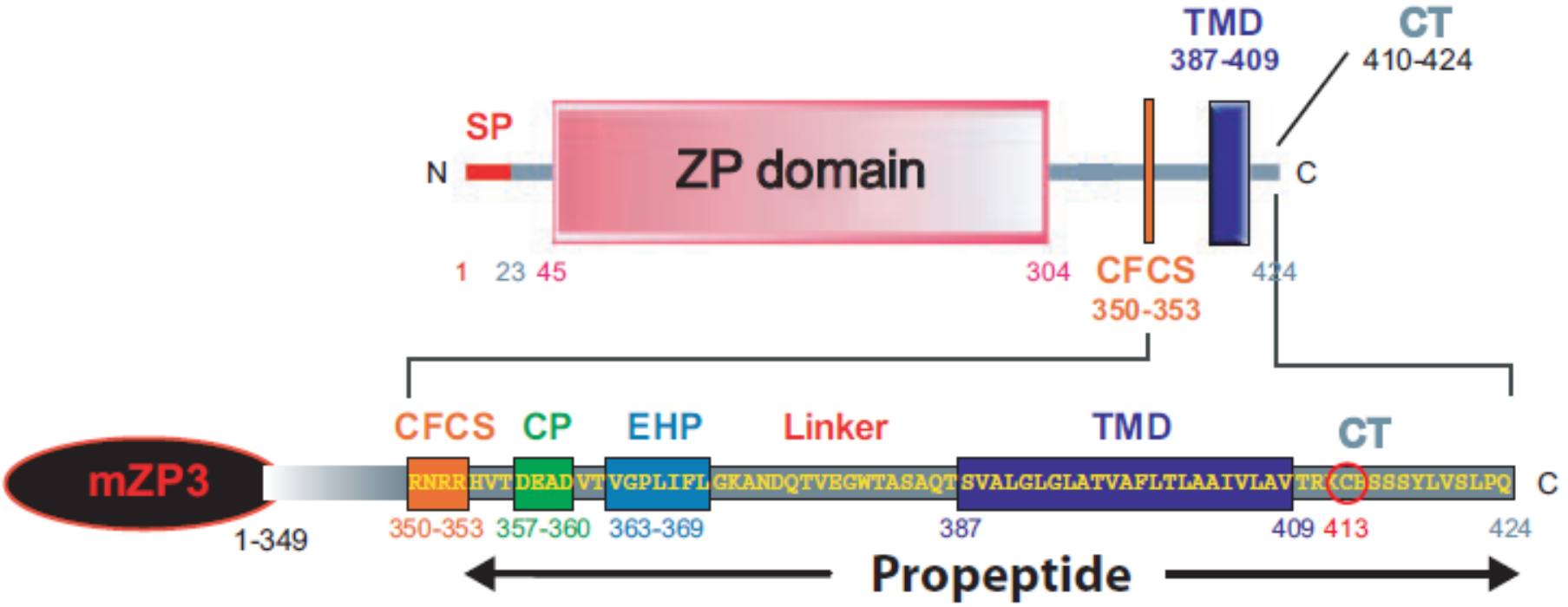
TMD
387-409
CT
410-424
SP
N
ZP domain
C
1 23 45
304
CFCS
350-353
424
CFCS
CP
EHP
Linker
TMD
CT
mZP3
RNRRHVTDEADVTVGPLIFLGKANDQTVEGWTASAQTSVALGLGLATVAFLTLAAIVLAVTRCCHSSSYLVSLPQ
C
1-349
350-353
357-360
363-369
387
409 413
424
Propeptide

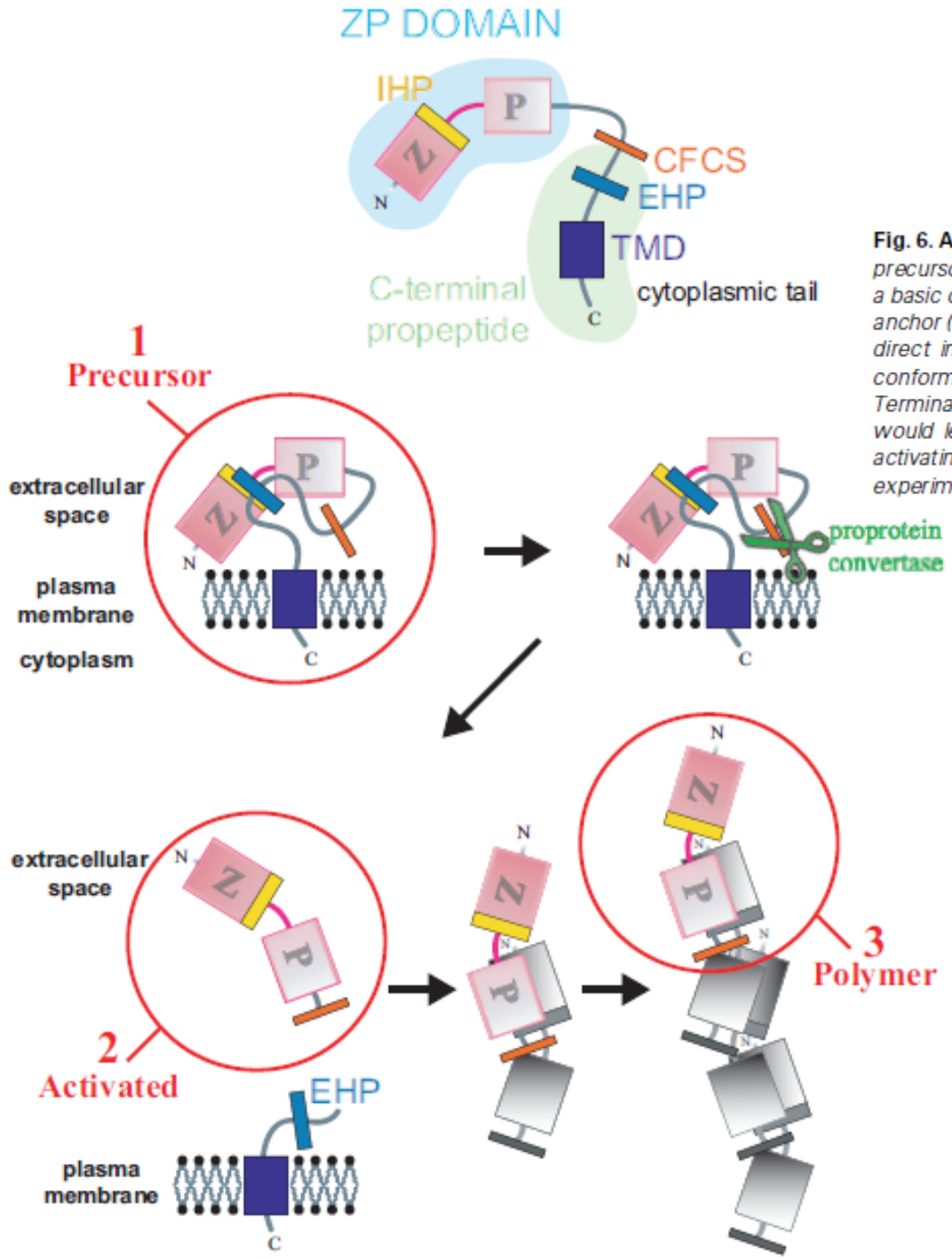

Fig. 6. A general mechanism for assembly of ZP domain proteins. *In all ZP domain precursors, the ZP domain is followed by a C-terminal propeptide (CTP) that contains a basic cleavage site (such as a CFCS), and EHP, and, in most cases, a TMD or GPI-anchor* (top panel)*. Precursors do not polymerize within the cell either as a result of direct interaction between the EHP and IHP or because they adopt an inactive conformation dependent on the presence of both patches* (middle left panel)*. C-Terminal processing at the CFCS by a proprotein convertase* (middle right panel) *would lead to dissociation of mature proteins from the EHP* (bottom left panel)*, activating them for assembly into filaments and matrices* (bottom right panel)*. For experimental details that led to this mechanism see Jovine* et al. *(2004).*

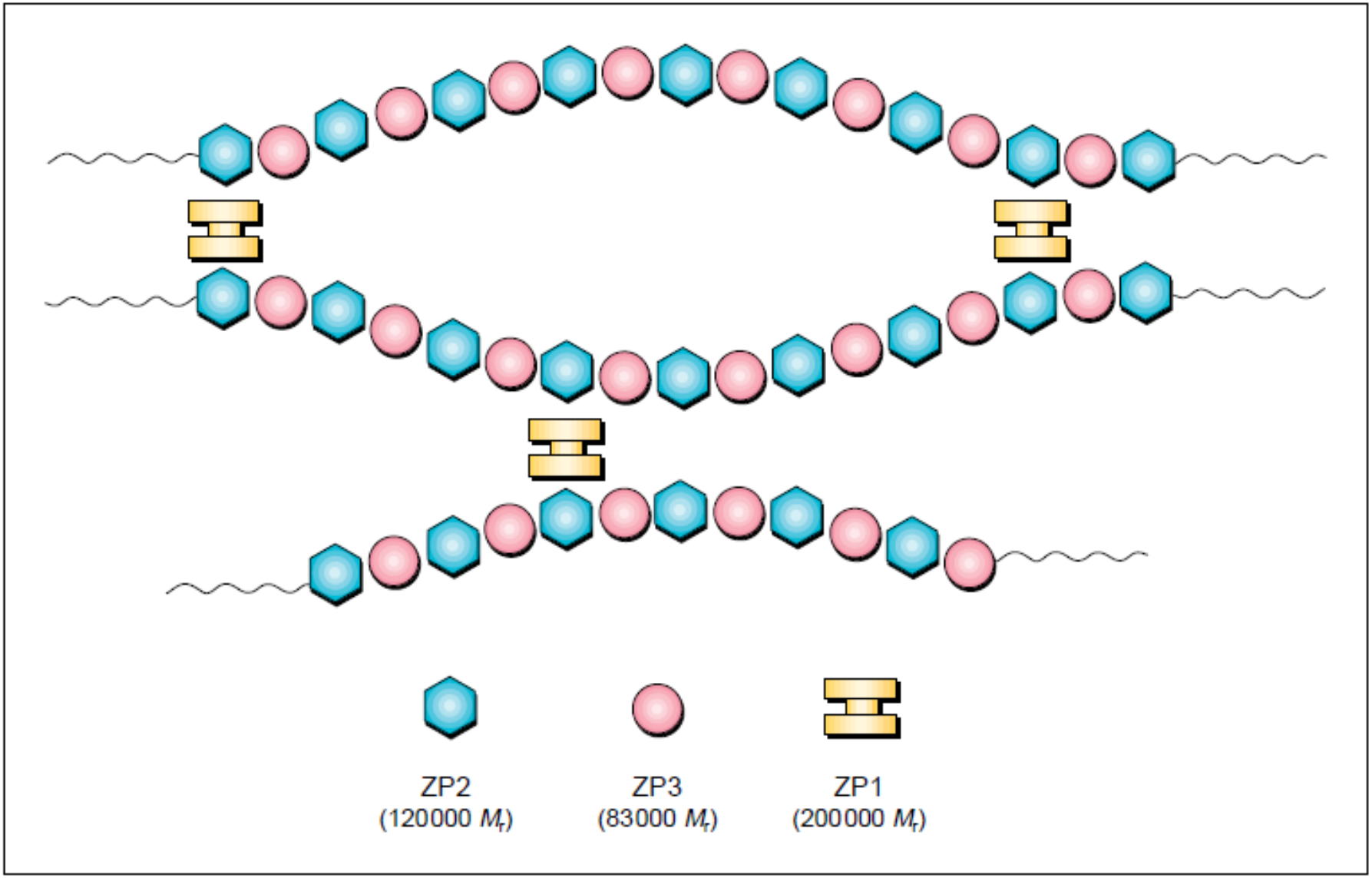

Fig. 1. The current model of the zona pellucida as proposed by Wassarman and redrawn from Wassarman (1988). Filaments are constructed of repeating ZP2–ZP3 units and are cross-linked by ZP1. Calculations of the ZP2:ZP3 ratio using recent sequence data confirm that it is close to 1:1. Although the model is consistent with experimental observations, formal proof that the zona pellucida is constructed in this way is still lacking. It is unclear whether ZP1 binding sites are present on every ZP2–ZP3 dimer and, if so, how ZP1 cross-links are actually distributed.

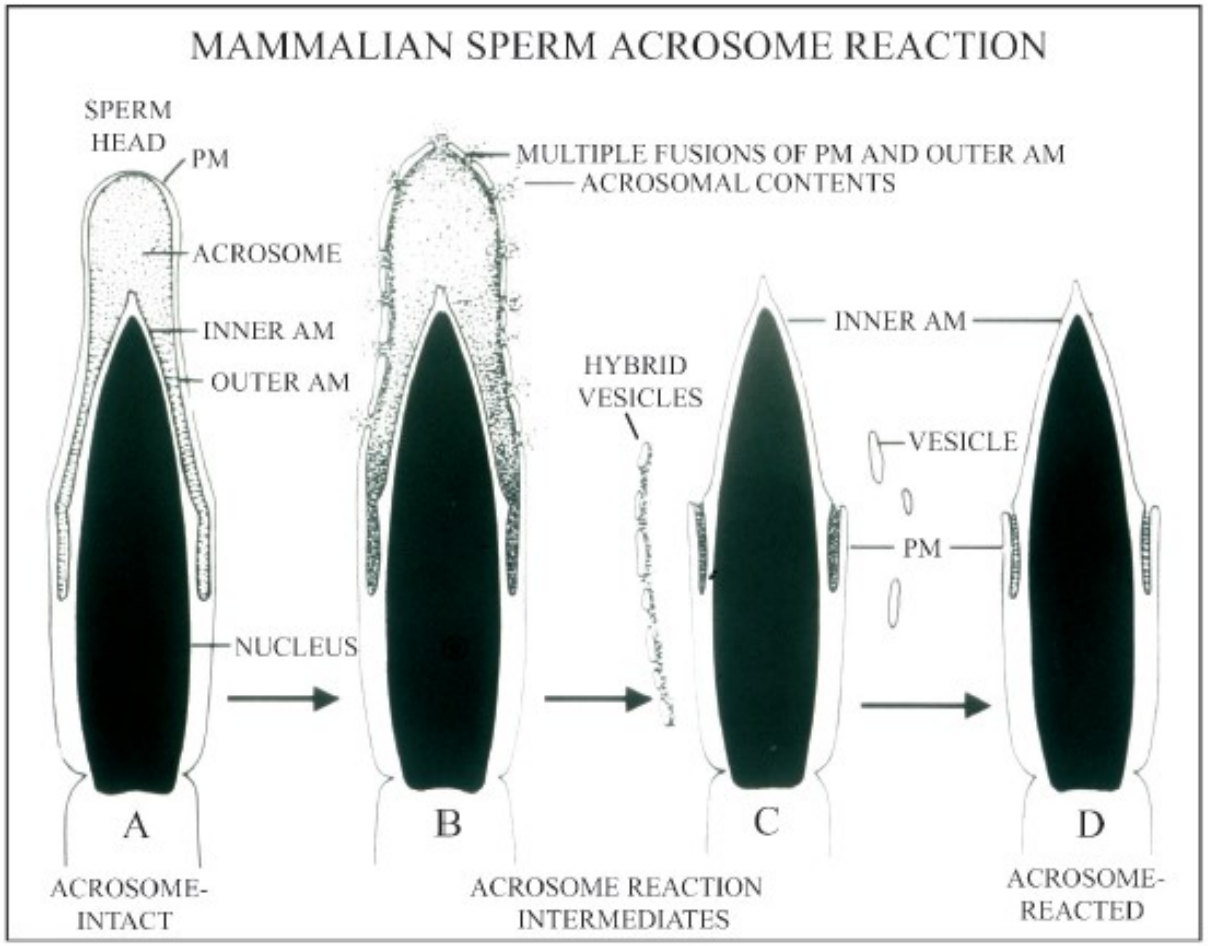

ZP3 stimulates several signal-transducing components in sperm, including: G proteins, IP3 and IP3 receptors, phospholipase C, voltage sensitive calcium channels.

- Activates G proteins (Gi1, Gi2, Gq/11)
- Depolarizes plasma membrane (-60 to -30 mV)
- Increases intracellular pH (by 0.3 units)
- Increases intracellular [calcium] (from 150 to 400 nM)

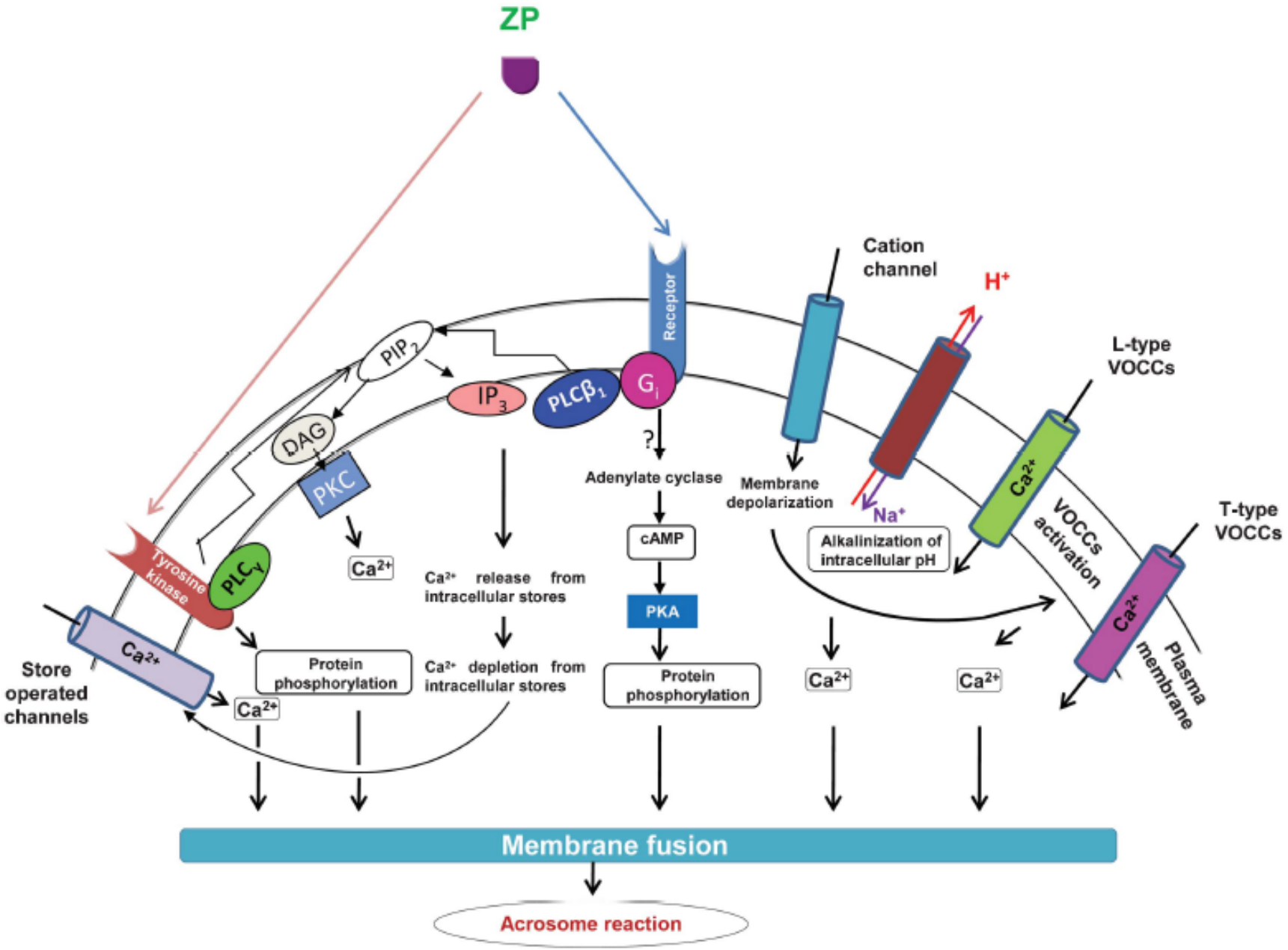
ZP
Receptor
Cation channel
H+
L-type VOCCs
PIP2
IP3
PLCβ1
Gi
?
DAG
PKC
Adenylate cyclase
Membrane depolarization
Na+
Ca2+
VOCCs activation
T-type VOCCs
Tyrosine kinase
PLCγ
Ca2+
cAMP
Alkalinization of intracellular pH
Ca2+ release from intracellular stores
Store operated channels
Protein phosphorylation
Ca2+ depletion from intracellular stores
PKA
Protein phosphorylation
Ca2+
Ca2+
Ca2+
Plasma membrane
Membrane fusion
Acrosome reaction

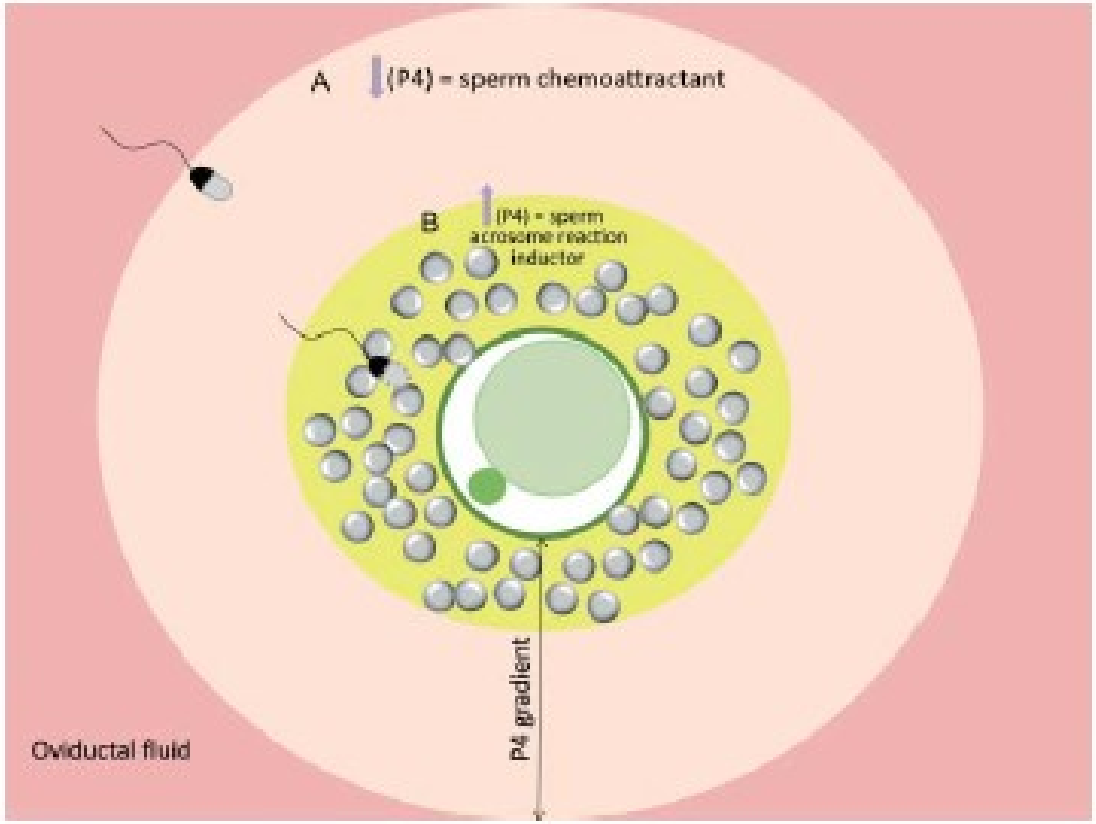

Figure 5 Progesterone (P_4) levels close to the fertilization location and its effect on sperm. (A) Low P_4 levels acting like a chemoattractant driving the sperm toward the oocyte. (B) High P_4 levels secreted by cumulus cells induce acrosome reaction.

Membrane depolarization

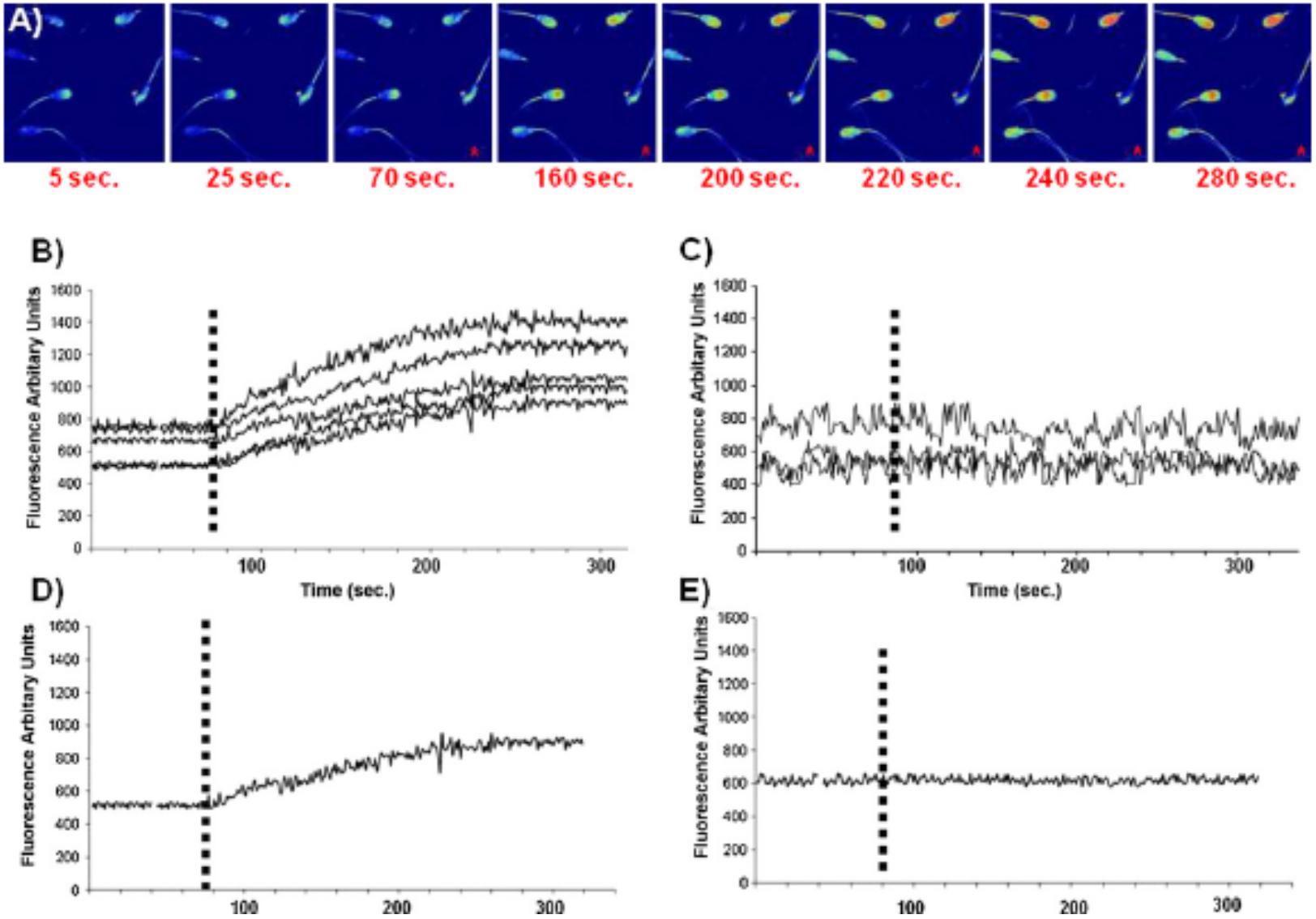

Calcium peack

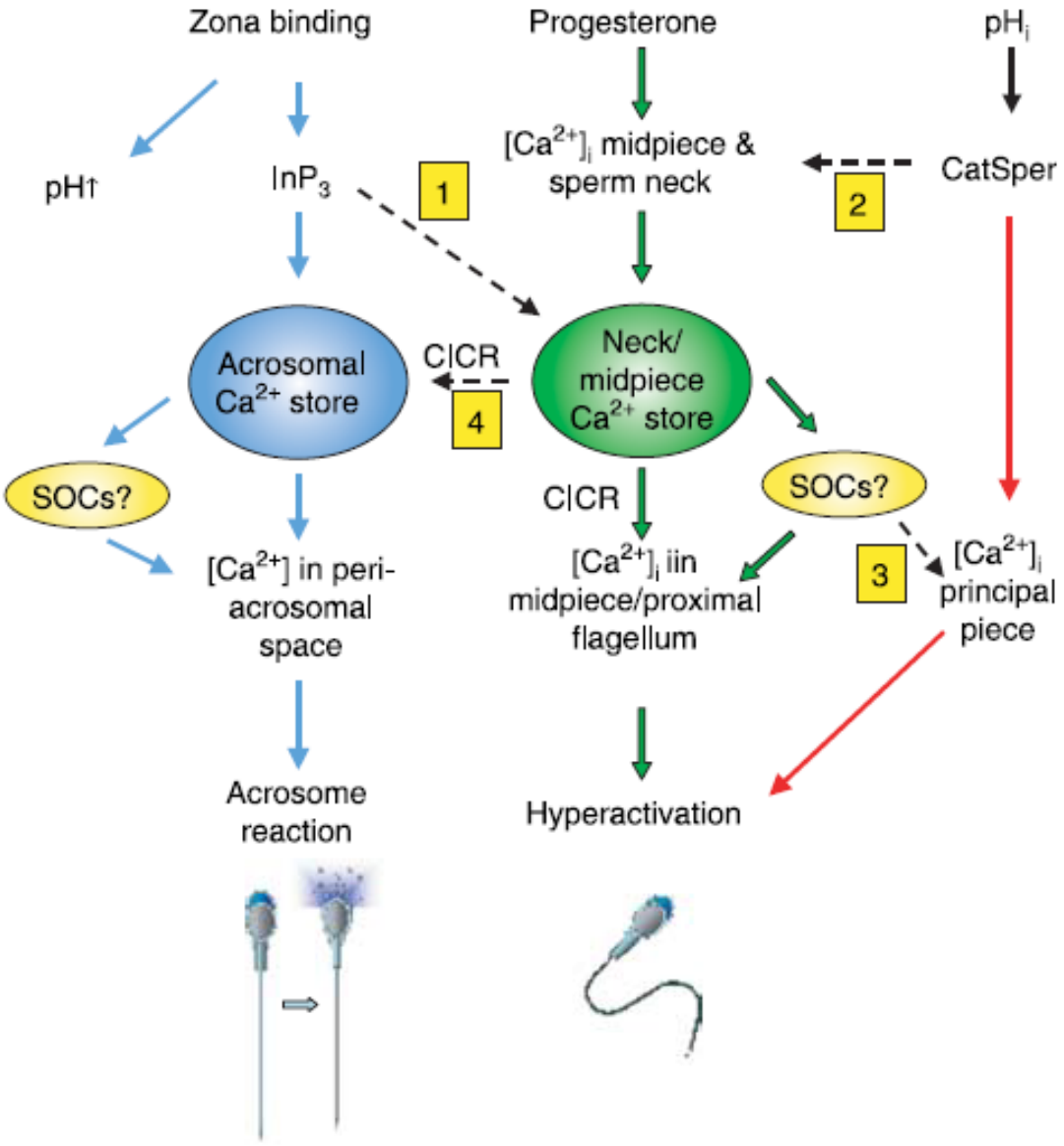

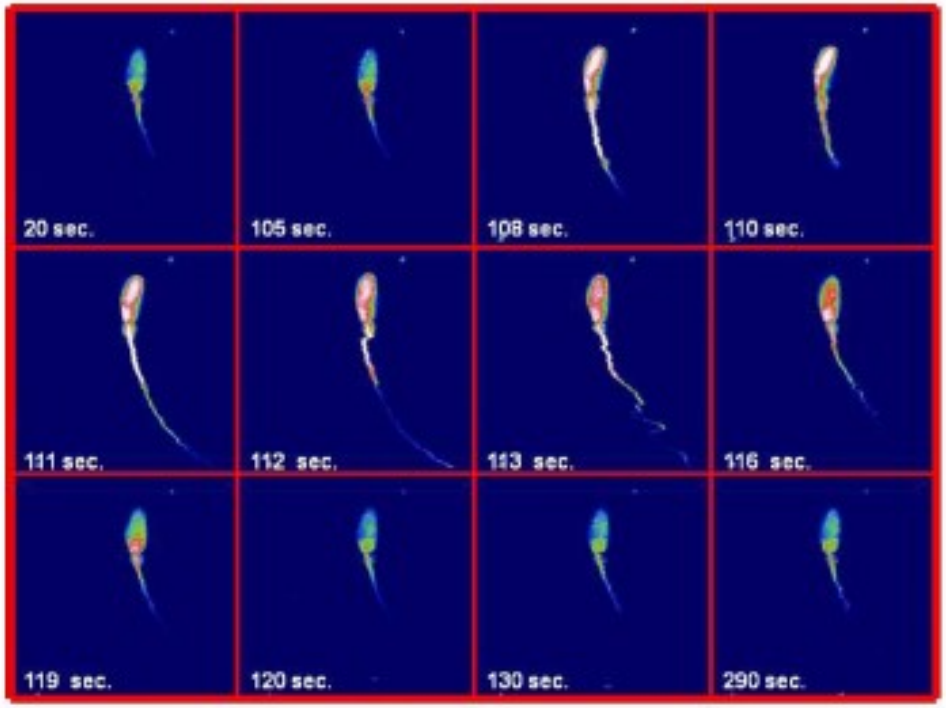

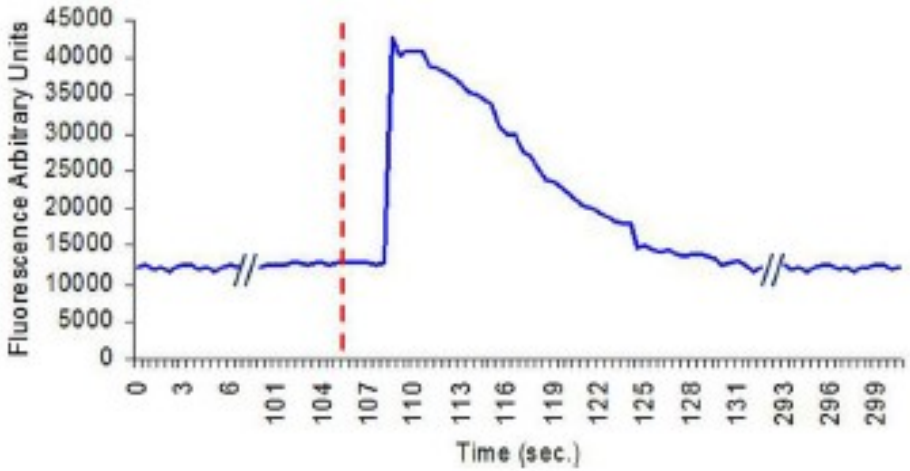

Figure 9 An example of confocal image gallery of CD treated spermatozoa loaded with Fluo-3AM exposed to sZP. An example of confocal image gallery of CD treated spermatozoa loaded with Fluo-3AM exposed to sZP (vertical red line). Notice that the rise in the $[Ca^{2+}]_i$ in spermatozoon is evident after <10 sec. from sZP addition, whereas return on the baseline occurs after about 30 sec.

Cytosckeleton dynamics

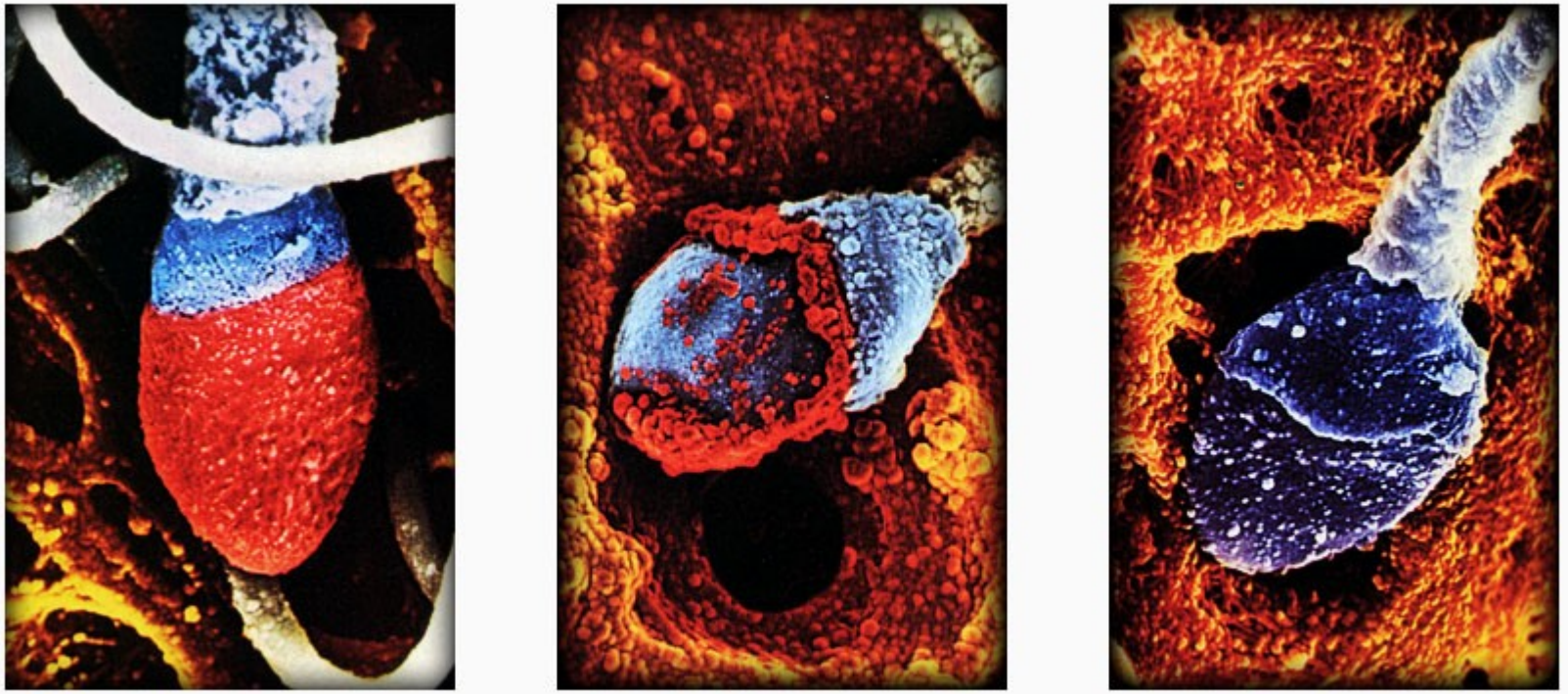

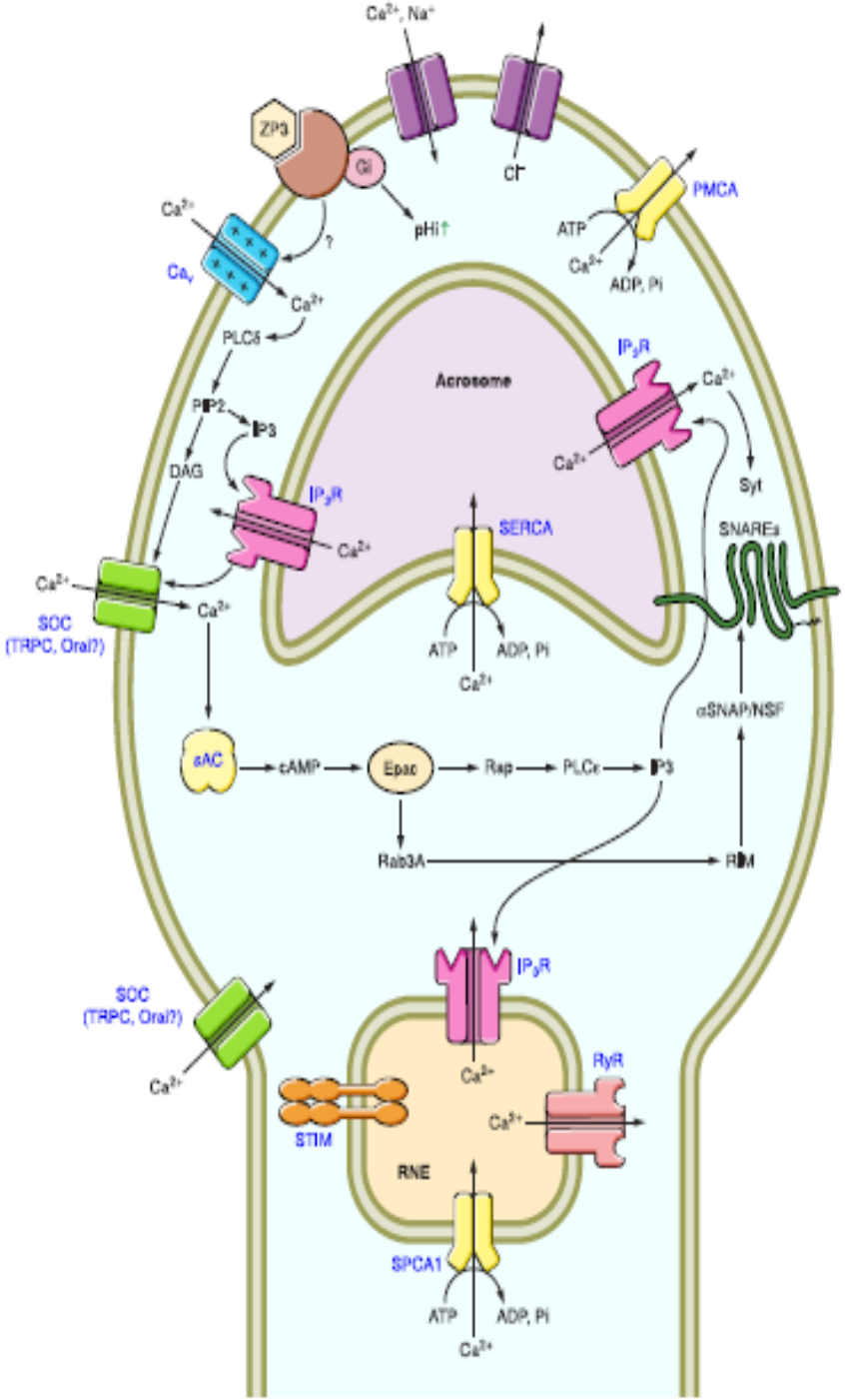
Ca2+, Na+
Cl-
ZP3
Gi
pHi↑
?
Ca2+
Cav
Ca2+
PLCδ
PIP2
IP3
DAG
IP3R
Ca2+
Ca2+
SOC
(TRPC, Orai?)
Ca2+
Acrosome
SERCA
ATP
ADP, Pi
Ca2+
PMCA
ATP
Ca2+
ADP, Pi
IP3R
Ca2+
Ca2+
Syt
SNAREs
αSNAP/NSF
sAC
cAMP
Epac
Rap
PLCε
IP3
Rab3A
RIM
IP3R
Ca2+
SOC
(TRPC, Orai?)
Ca2+
RyR
Ca2+
STIM
RNE
SPCA1
ATP
ADP, Pi
Ca2+

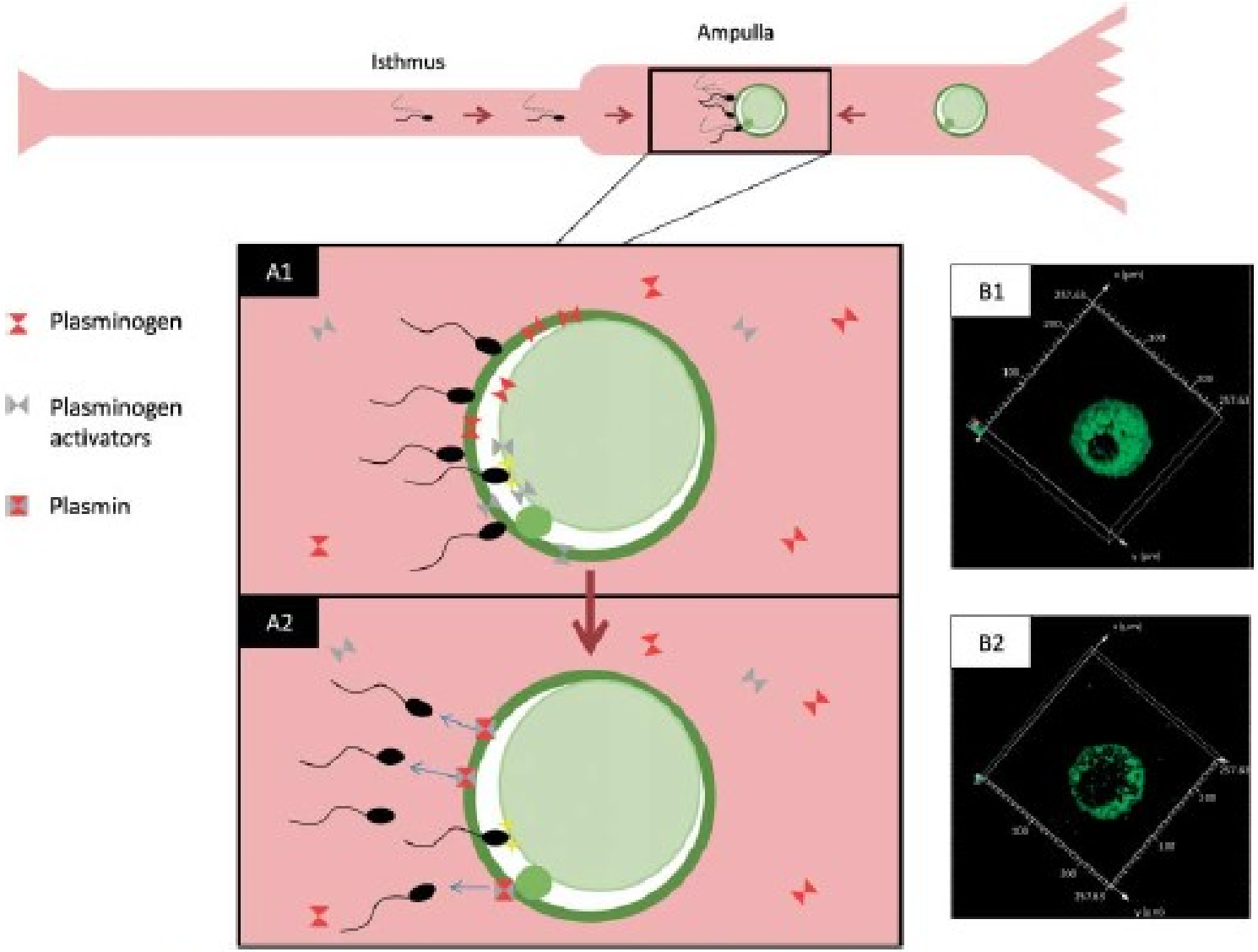

Figure 6 Proposed model for the role of the plasminogen–plasmin system during fertilization. Plasminogen and plasminogen activators are present in the oolemma and ZP of the oocyte (A1). Oocyte immunostaining with antibodies against plasminogen activators shows the oolemma strongly labeled (B1). When the spermatozoa bind the oolemma, plasminogen activators are released and increase the activation of the plasminogen into plasmin. Plasmin detaches additional spermatozoa bound to ZP (A2). The labeling in the oolemma decreases a few minutes after sperm binding (B2).